A UNITED STATES DEPARTMENT OF COMMERCE PUBLICATION

NOAA Technical Report ERL 194-AOML 4

U.S. DEPARTMENT OF COMMERCE
National Oceanic and Atmospheric Administration
Environmental Research Laboratories

Some Tests on the Radiosonde Humidity Error

FEODOR OSTAPOFF
WILLARD W. SHINNERS
ERNST AUGSTEIN

BOULDER, COLO.
DECEMBER 1970

U.S. DEPARTMENT OF COMMERCE
Maurice H. Stans, Secretary

NATIONAL OCEANIC AND ATMOSPHERIC ADMINISTRATION
Robert M. White, Acting Administrator
ENVIRONMENTAL RESEARCH LABORATORIES
Wilmot N. Hess, Director

NOAA TECHNICAL REPORT ERL 194-AOML 4

Some Tests on the Radiosonde Humidity Error

FEODOR OSTAPOFF

WILLARD W. SHINNERS

ERNST AUGSTEIN

ATLANTIC OCEANOGRAPHIC AND METEOROLOGICAL LABORATORIES
MIAMI, FLORIDA
December 1970

For sale by the Superintendent of Documents, U. S. Government Printing Office, Washington, D. C. 20402
Price 55 cents.

TABLE OF CONTENTS

SOME TESTS ON THE RADIOSONDE HUMIDITY ERROR

Feodor Ostapoff

Willard W. Shinners

Ernst Augstein[1]

Humidity data obtained from carbon hygristors flown in radiosondes used by United States meteorological services in low latitudes may have significant errors due to solar heating. Specially modified radiosondes to block solar radiation were flown simultaneously with unmodified radiosondes to determine the magnitude of the error. Additional tests were made in a vertical wind tunnel to check ventilation rates of the hygristor and a temperature/humidity chamber was used to simulate environmental conditions and to verify the temperature dependence of the sensor. A correction curve for application to ATEX daytime data was developed and compared with a similar curve based on comparison flights between the German radiosonde M60 and the U. S. 403 MHz radiosonde. These latter tests were made in the Equatorial Atlantic in March 1969. Independent tests of the proposed corrections were applied to data obtained during July and August 1970 in the sub-tropical Atlantic with good results.

1. INTRODUCTION

Recently, a number of field experiments were conducted in tropical regions, notably the Line Island Experiment, the Atlantic Trade Wind Experiment (ATEX), and the Barbados Oceanographic and Meteorological Experiment (BOMEX). Examination of the radiosonde humidity data has shown a pronounced diurnal variation. To investigate this diurnal variation of humidity, the NOAA (formerly ESSA) Sea-Air Interaction Laboratory (SAIL)

---

[1] Meteorological Institut of the University of Hamburg, Hamburg, Federal Republic of Germany.

conducted a series of tests in the spring of 1970 with the prime objective of developing a correction procedure for the day flights made during ATEX. Therefore, the environmental tests were made under typical trade wind conditions and the analysis concentrated on the errors in the moist layer under the trade wind inversion. Data from simultaneous German/U.S. radiosonde flights made on board the R/V *Meteor* in equatorial waters were analyzed at the University of Hamburg for the apparent error.

Three possible error sources may be attributed to the present configuration of the U. S. radiosonde. The first, and probably the largest, error results from solar radiational heating of the carbon humidity element which is mounted in a horizontal channel on top of the radiosonde box under a precipitation shield that is translucent to sunlight. This has an effect of warming the carbon strip that is a nearly perfect absorber of at least short-wave radiation and consequently will operate at a higher temperature than the indicated environmental air temperature (Morrissey and Brousaides, 1970). The increased temperature of the surface of the carbon element heats the air contacting the element's surface, thus increases its saturation vapor pressure, with lower relative humidity (RH) indicated.

Second, the pulse type 403 MHz radiosonde has the transmitter in the compartment below the hygristor, whereas the AM 403 MHz sonde has only the baroswitch in the compartment and the battery and transmitter below. Both the transmitter and battery represent a heat source. The lower surface of the humidity duct emits infrared radiation that could be absorped by the carbon element, resulting in a higher sensor temperature than the ambient air temperature. Since the emissivity of the radiosonde plastic housing is small, we expect that the heating caused by this effect remains relatively low.

Third, due to the peculiar duct configuration the rate of ventilation is different than the rate of ascent of the radiosonde. Reduced ventilation rates will prolong the time constant and increase the temperature difference between the actual air temperature and the carbon element, as a result of the atmospheric lapse rate.

This report describes the efforts made by SAIL to assess the magnitude of these errors in humidity measurements, when using the present radiosonde. Temperature and RH data for the experimental observations made at Miami are in appendix A.

2. ENVIRONMENTAL TESTS

The total effect of such errors can be seen in figure 1, which shows the diurnal variation of specific humidity. Curve 1 was derived from 4 weeks of radiosonde data (German M60 model) obtained on R/V *Meteor* in the southeast trade wind regime in 1965. The specific humidities of eight ascents a day were averaged between 150 and 1000 m. A minimum is reached before sunrise and a maximum shortly after local noon. The amplitude amounts to about $\pm$ 0.3 g/kg. Curve 2 represents a 4 day average of specific humidities obtained in 1969 on U. S. C&GS Ship *Discoverer* during ATEX using U. S. 403 MHz radiosondes. Each value is a mean between 200 and 700 m, i.e., well in the moist layer below the trade wind inversion. The amplitude is almost one order of magnitude higher and the distribution of the maximum and minimum is 180° out of phase when compared with curve 1.

Thus, it is apparent that at least the daytime humidity values obtained during the ATEX operation contain considerable errors, so we began a test program to assess the magnitude of the different errors. First, the radiosonde ascents in the

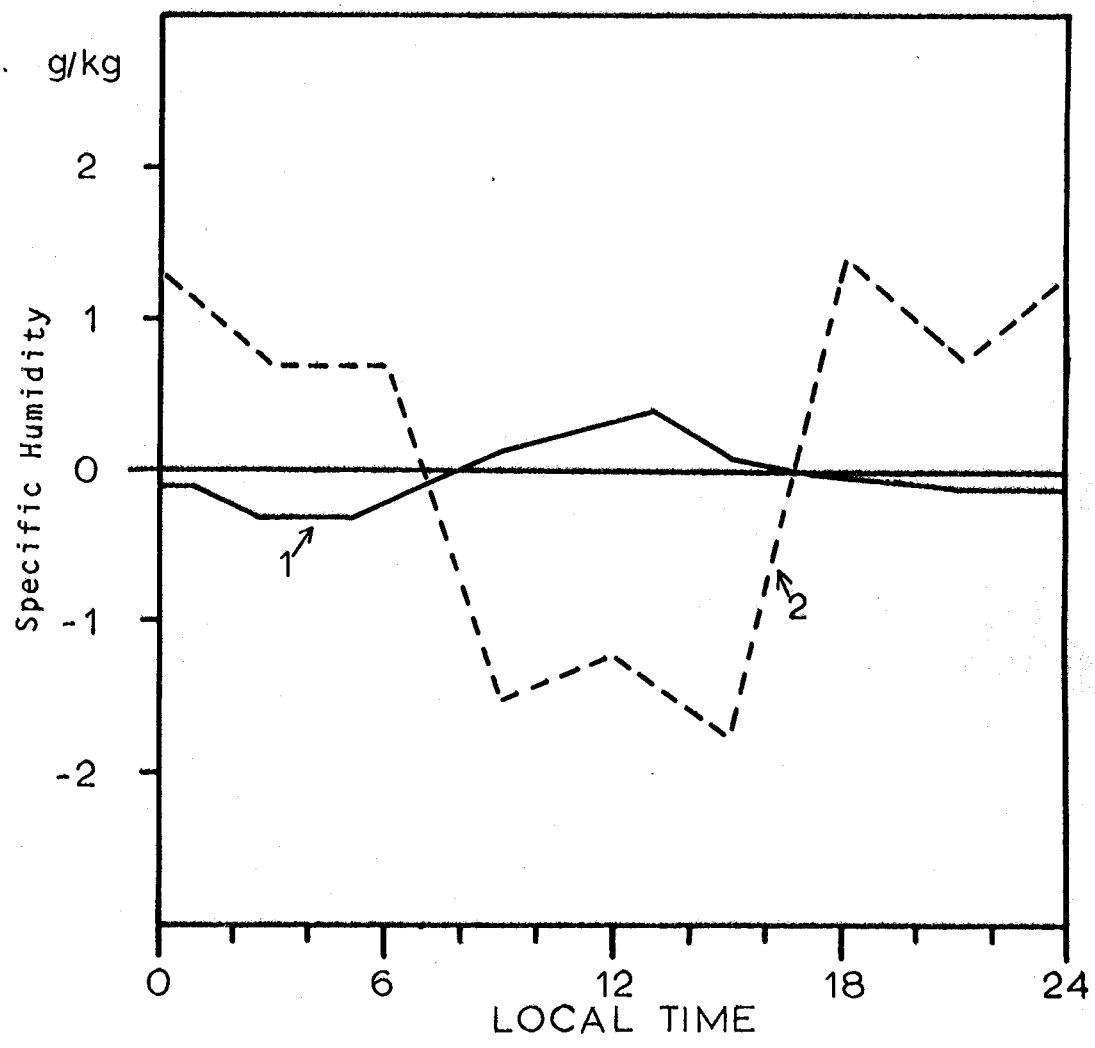

Figure 1. Diurnal variation of the mean specific humidity in the moist layer below the trade wind inversion (curve 1). Curve 2 shows uncorrected specific humidities obtained during ATEX (see text).

Miami area were compared to establish as well as possible the total error and to use these data to provide corrections to existing data.

The majority of tests were made during typical fair-weather cumulus conditions that represent the undisturbed trade wind regime, although some were made during cloudy conditions and at night.

The standard pulse type 403 MHz radiosonde was compared with modified versions that, we believe, have significantly reduced the radiation error caused by solar heating.

There were two types of modifications, the first type consisted of a minimal change and could be accomplished within a few minutes. Adhesive aluminum foil was placed on the top of the humidity duct to block the transmission of solar radiation, the inside of the duct was sprayed with black paint (nonglossy) to prevent scattered and reflected radiation from reaching the black carbon element (see fig. 2).

The second modification was more drastic because the duct was completely reconfigured. Since there was no intention to fly the sondes in conditions of active precipitation, a vertical tube was attached to the radiosonde. It was manufactured from 1/4-inch styrofoam and covered on the outside with adhesive aluminum foil. The inside of the duct was sprayed with black, nonglossy paint except for the top 2 inches, which were left white. The sensors were in the lower third of the tube (see fig. 3) where they were shielded from radiation and had excellent ventilation. This modification was used for all comparison flights

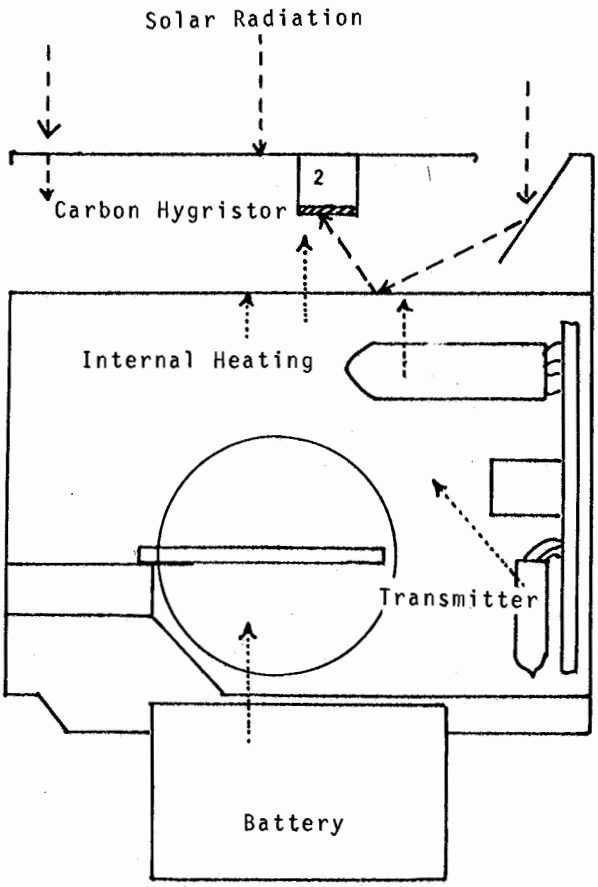

Figure 2. Diagram of the 403 MHz radiosonde with probable sources of heating of the hygristor at 2.

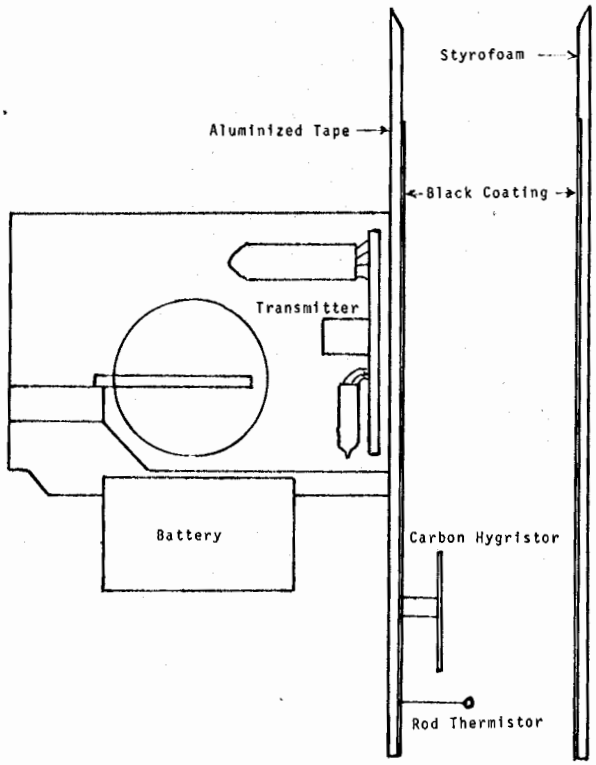

Figure 3. Radiosonde modified to minimize solar and internal heating of the hygristor.

except the one on February 10, 1970, in which aluminum foil was used over the hygristor and a flight on February 16, 1970 that intercompared both modifications.

The following procedure was established for all of these flights. Each flight train consisted of a 600 g balloon inflated to give at least a 300 m per minute rate of ascent, a parachute, a train regulator, a standard WB 403 MHz pulse modulated sonde, and a modified sonde, as described above (was below the standard). In general, the standard sonde was transmitting on the off-set frequency of 407 MHz, and the modified sonde was transmitting on 403 MHz. On the ground two receivers recorded the respective sondes and the two recorders were synchronized closely by time tics.

On several flights the position of the sondes on the train was reversed to determine whether relative position would cause any bias. None was apparent. The results of these flights are presented in the appendix.

2.1 Comparison Between the Standard and Minimum Modification Sondes

The modification consisted of covering the top with aluminum foil and of blackening the duct (from here on referred to as alu-modification). This minimum modification indicates that the largest error contribution comes from direct radiational heating. For example, at 900 mb the alu-modification sonde records RH values 10 percent higher than the standard sonde. Therefore, an ascent was made that compared the alu-modification with the vertical duct type modification. On the average, the difference did not exceed 5 percent RH with the duct type sonde recording still higher RH values during high humidity conditions (surface to 960 mb, 760 to 680 mb) and lower RH at low RH values (940 to 750 mb). This indicates that the better ventilation of the vertical duct improves the response time of the sensors. This effect is discussed later in section 3.3. All further test flights were made with the vertical duct modification.

2.2 Comparison Flights Between Standard Sondes and Vertical Duct Sondes

These comparison flights were made under various day and night conditions. An example of typical trade wind conditions on February 19, 1970, may be found in the appendix. A temperature inversion of 6°C between 910 mb and 880 mb acts as a lid on the moist layer. Below the inversion the standard radiosonde reported 70 percent RH while the modified duct sonde showed 90 percent RH, a difference of 20 percent RH or from 9.1 g/kg to 7.0 g/kg in corresponding mixing ratio. Similar results can be found in the other daytime observations (see appendix).

These latter ascents from April 18 to April 24, 1970, were performed somewhat differently in order to obtain simultaneous humidity readings. In the earlier flights, due to small differences in the baroswitches of the two sondes, one sonde reported temperature while the other reported humidity or reference. The modified duct type sonde was rewired to report humidity continuously, interrupted only by the reference signal at every fifth contact point. Hence, the appendix also shows values of RH that were measured exactly at the same time. These tests were made to obtain sufficient simultaneous data to develop the correction procedure (see sec. 5) that will be applied to the ATEX data.

As expected, flights during thick overcast conditions and at night showed little humidity differences or nearly identical readings between the two sondes (within the sensor accuracies).

All data are presented in the appendix.

3. LABORATORY TESTS

Several tests were made in the laboratory. Due to limited resources these tests should be considered as only providing rough estimates of some other possible errors not directly attributable to solar heating. For these tests a 6-foot vertical chamber with a 2 foot x 2 foot cross section was built and was provided with fans to generate a vertical wind of about 5 m/sec, or the average rate of ascent of a radiosonde.

3.1 Electronic Heating

The radiosonde was placed in the vertical wind tunnel with thermocouples at basically two places. Continuous temperature readings were obtained, from the center of the entrance to the humidity duct of the regular radiosonde and from the

carbon element itself. A thermocouple junction was attached to the carbon element and covered by a drop of silicone grease. At the same time dry- and wet-bulb temperatures were measured in the vertical wind tunnel some 12 inches above the suspended radiosonde for control purposes.

The battery was activated and the radiosonde was prepared in the same way as before actual releases. The measurements started 30 min after the radiosonde was activated, a normal time span for baseline checks and flight preparation. The tests ended after 2 hours of operations. No attempts were made to test the radiosondes under other than surface atmospheric pressure. The ventilation effect under reduced atmospheric pressure is not known.

A number of different radiosondes were tested, which included the types used during BOMEX. Although these sondes differ in transmitting frequency and location of battery or transmitting electronics, they all have the same configuration as far as the humidity sensor exposure is concerned. Also, the plastic material of the radiosonde housing, is the same. Table 1 shows the results.

Also, some tests were made by changing the temperature of the air flow to determine the temperature time lag of the carbon element (see sec. 3.2).

Finally, the modified vertical duct type radiosonde used for the environmental comparison flights (see sec. 2) was similarly tested and no heating effects detected.

Table 1. Heating of Hygristor in Various Radiosondes due to Electronics and/or Battery.

	Radiosonde Type			
	403MHz Pulse	403MHz AM	Transponder 1680/403MHz	72MHz
Temp. °C	+ 0.3	+ 0.4	+ 0.7	+ 0.2

3.2 Humidity Response Time of the Radiosonde System

Two separate attempts were made to determine the time constant of the humidity sensor under variable temperature conditions. For these tests the carbon element was removed from the radiosonde housing and exposed directly to the air stream. Temperatures (and in one experiment the RH) were changed, with the resistance change of the carbon element being transmitted to the radiosonde receiver and recorded conventionally on the strip chart recorder. The experimental set-up for the first series of tests is shown in figure 4. Two different air masses were available. The laboratory air had a temperature of about 20°C and a relative humidity of 48 percent. A large storage box was supplied with air from an air conditioning duct having a temperature of about 10°C and a RH of 68 percent. The air was drawn at about 5 m/sec by a fan through a channel containing the carbon element and a number of thermocouples. Temperature and humidity were observed in the cold storage box by calibrated mercury thermometers. Figure 5 is an example of a typical humidity trace. The ventilation rate at the sensor was 5 m/sec. It is clearly evident that when the cold air comes in contact with the carbon element the recorded "RH" drops at first by roughly 5 percent and after about

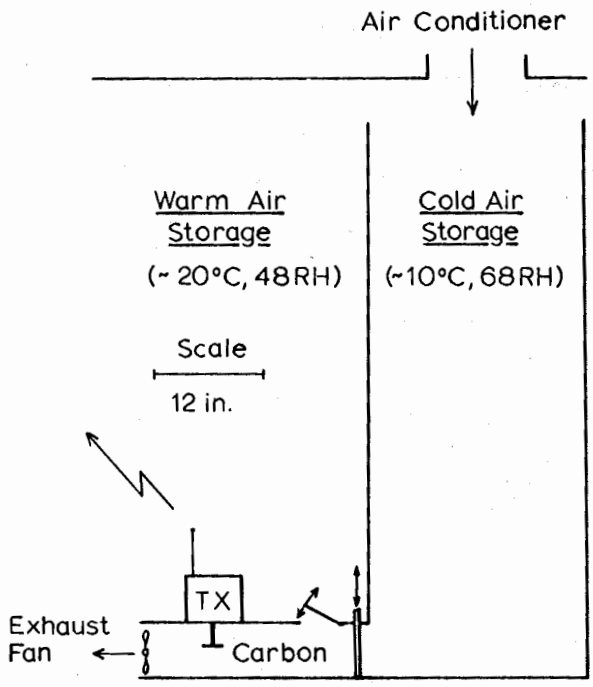

Figure 4. Experimental arrangement for response time determination.

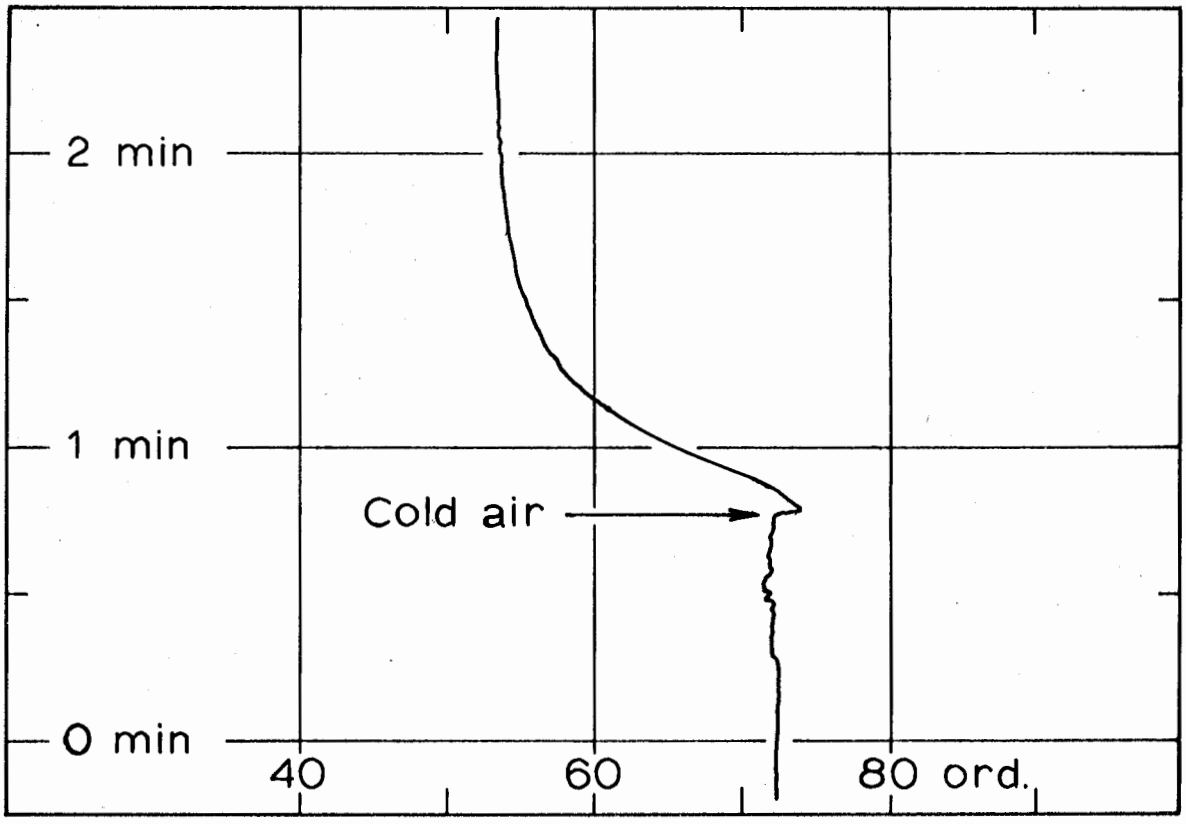

Figure 5. Apparent humidity decrease during rapid temperature decrease at 5 m/sec ventilation rate.

5 sec acquires its original value. The time constant was determined as the time required to attain 64 percent of the new value. An average value of 17 sec was observed at 5 m/sec ventilation rate. However, at 1.5 m/sec the time constant increased to 45 sec (see fig. 6). These are approximate values because the time constant was determined from the recorded signal without taking the nonlinearity of the resistence vs. RH curve into account (Marchgraber and Grote, 1965). However, the error may not be exceedingly large because between 50 percent RH and 65 percent RH this relationship can be approximated to the first order by a straight line.

This preceeding test involved two air masses with both parameters, temperature and humidity, changing. The experiment

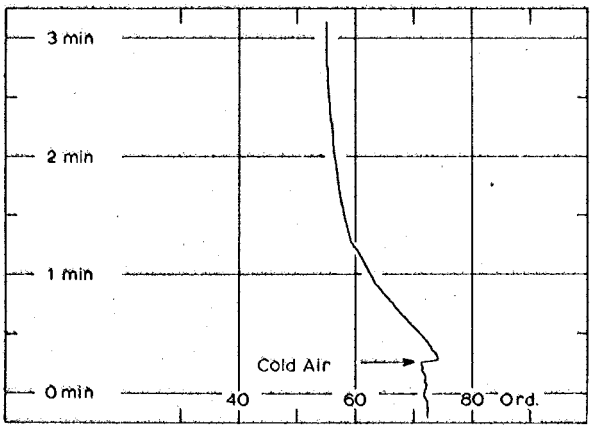

Figure 6. Apparent humidity decrease with sudden temperature drop at 1.5 m/sec ventilation rate.

was repeated by attempting to create two air masses differing only in temperature and with identical RH. This was accomplished by means of an environmental chamber. The experimental arrangements are outlined in figure 7.

The air in the environmental chamber was heated to several degrees above room temperature while the RH was kept equal to that in the room. A small fan kept the air circulating rapidly. Temperature, humidity (by means of carbon element), and air movement (hot wire anemometer) were monitored. Adjacent to the chamber, a horizontal duct was placed containing another carbon element, temperature gauge, and hot wire anemometer. When RH_1 (room humidity) equalled RH_2 (chamber humidity), the chamber cover was removed rapidly and room air with $T_1 < T_2$ was blown at a speed of about 5 m/sec over the carbon element in the environmental chamber. Again, the signal from the carbon element was

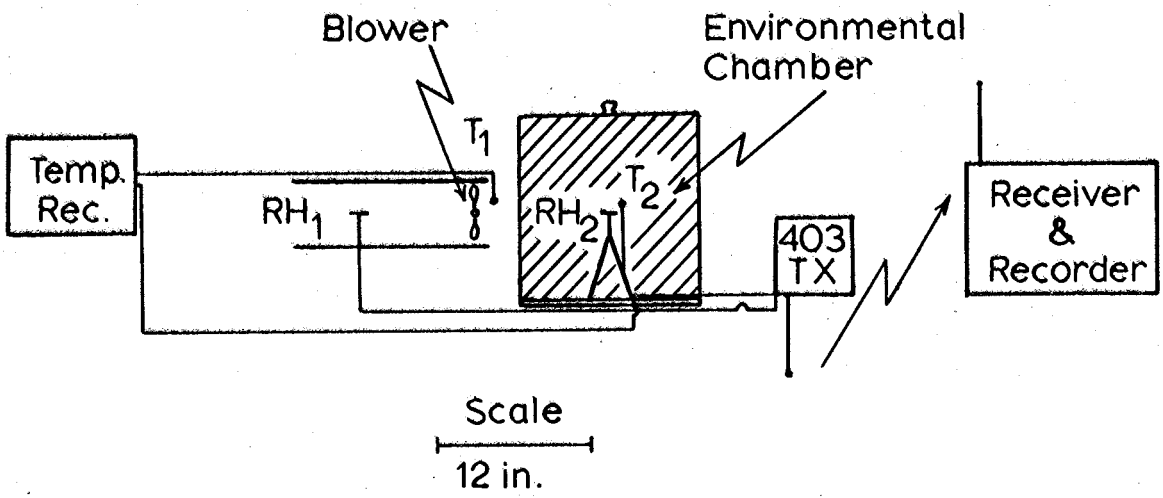

Figure 7. Experimental arrangement for response time with the same temperature but different humidities.

transmitted from a 403 MHz transmitter to a nearby receiver and recorded by the radiosonde recorder. Figure 8 shows an example of these tests. This second test confirmed the findings of the previous tests, namely, a time constant of the humidity radiosonde system of about 16 sec, if a ventilation rate of 5 m/sec is maintained.

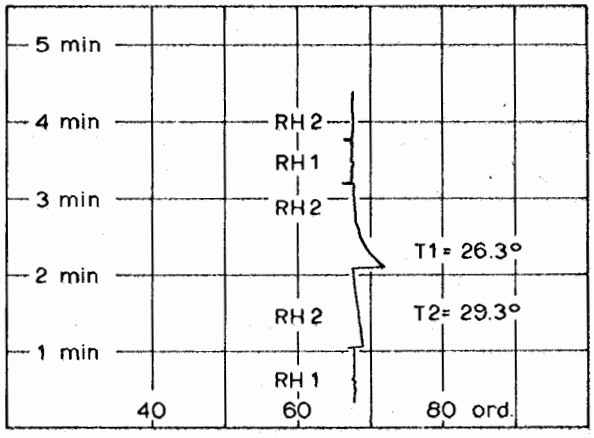

Figure 8. Record for tests with equal relative humidity and different temperatures.

For this test two different air masses were generated with the following properties:

	T (°C)	RH (%)	$e_s(T)$ (mb)	e_a (mb)
air mass 1	29.3	50	40.755	20.378
air mass 2	26.3	50	34.209	17.105

The carbon element is held in air mass 1 until thermally adjusted. When suddenly exposed to air mass 2, the element will acquire the new temperature very slowly due to its heat capacity. Therefore, in the close vicinity of the element the saturation water vapor pressure e_s (at T = 29.3) will change at a rate similar to the thermal property of the element. Hence, at the time of air mass 2 arriving at the element, the RH is given by the ratio

$$\frac{e_a(\text{air mass 2})}{e_s(T = 29.3°C)} = \frac{17.105 \text{ mb}}{40.755 \text{ mb}} = 42\% \text{ RH}.$$

This means that under these test conditions because of the 3°C higher surface temperature of the carbon element, the recorded relative humidity will be 8 percent lower than the actual humidity associated with air mass 2.

In this test a reduction of RH by 9 percent was found (see fig. 8) thus confirming the expected effect. Furthermore, the test shows that the actual time constant of the carbon element measuring RH is determined primarily by the effect of changing temperature, which is quite different from the time constant of the carbon element at constant environmental temperatures. Furthermore, if 3°C/300 m is the average lapse rate and the balloon's rate of ascent is 300 m/min, the temperature change experienced by the radiosonde is $\frac{\Delta T}{\Delta t} = 3°C/$ min.

Also, if the thermal time constant of the carbon element is approximately 20 sec, the carbon element will be operating thermally at approximately 1°C higher temperature than the environmental temperature.

The apparent reduction in the humidity reading can be calculated for an air parcel with 80 percent RH and 22°C as follows:

$$\frac{e_a(21°,\ 80\%)}{e_s(22°,\ 100\%)} = \frac{19.889}{26.430} \simeq 75\%\ \text{RH}$$

resulting in an underestimate of 5 percent in RH value. This effect should be present in day and night flights due to the heat capacity of the carbon element.

3.3 Flow Rate Tests

To provide some estimates about the ventilation rate in the standard radiosonde humidity duct, we suspended the radiosonde housing in the vertical chamber and measured air speed with two hot-wire anemometer probes (TSI model 1051-2,

with linearized output). Figure 9 shows the locations, numbered 1 through 5, where wind speeds were measured. The reference speed was obtained 6 inches above the radiosonde housing. At this reference height, wind observations were made all across the chamber (24 inches by 24 inches) and no appreciable variation was found except very close to the chamber walls.

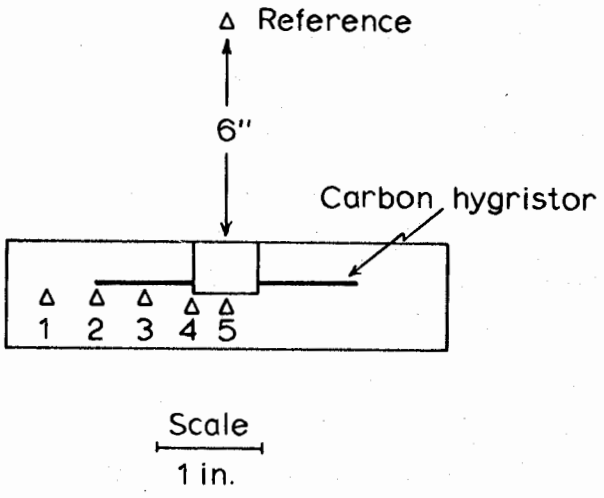

Figure 9. Cross section of humidity duct showing location of hot wire anemometer probes at points 1, 2, 3, 4, and 5. Air flow is toward the reader.

The results of the measurements are summarized in table 2. Each value represents percentage of flow reduction with respect to the reference speed. Each location had a mean of about 10 observations.

These tests seem to indicate that due to the peculiar configuration of the humidity duct the ventilation rate may be reduced to about 30 percent of the assumed rate of ascent. Normally, the balloon is inflated in such a way that is rises 300 m per min or 5 m per sec. It is possible that the actual

Table 2. Measurements of Air Flow in Humidity Duct

Location	Average Flow Reduction (%)
1	71
2	65
3	67
4	70
5	72

ventilation rate may be as low as 1.5 or 2 m per sec. In addition, the radiosonde train swings as it rises, which may add further difficulty in estimating the true ventilation rate and its possible variation through the humidity duct.

The modified sonde that was used in the comparison flights described in section 2.2 was also subjected to these tests with the results indicating very little flow reduction (about 7 percent near the carbon hygristor location).

In view of the results on the time constant of the humidity recording system (see sec. 3.2), we may conclude that due to all these effects, such as the sensor temperature and sensor exposure, environmental conditions, and recording system, the actual time constant may be as large as 30 to 40 sec.

4. COMPARISON TESTS BETWEEN THE U.S. RADIOSONDE AND THE GERMAN RADIOSONDE

After ATEX in March 1969, the German research vessel *Meteor* anchored at the equator and 30°W longitude for 4 weeks to conduct primarily an ionosphere program in connection with the active sun year. During that time a comparison program was carried out consisting of the U.S. 403 MHz pulse type radiosonde and the German M60 radiosonde. Both were attached to the same balloon. A total of 10 daylight ascents and five nighttime ascents were made.

The German sonde differs considerably from the U.S. sonde, both in configuration and in sensor. The configuration for sensor exposure is similar to the modified U.S. sonde used in the Miami comparison flights. As the humidity sensor, a rolled human hair is used, which is described by H.G. Muller (1965). Presumably, its characteristics at temperatures above

freezing and at high humidities are quite good, and it deterioriates quickly at -55°C. Between 0°C and -20°C the time constant increases which, according to Muller, is 10 sec for high humidities and temperatures above 0°C.

The data were grouped in four categories: (1) humidity data above 0°C, (2) humidity data below 0°C, (3) daylight flights, and (4) night flights. Figure 10 shows the relative frequency distribution at daytime (1000 local time) and temperatures

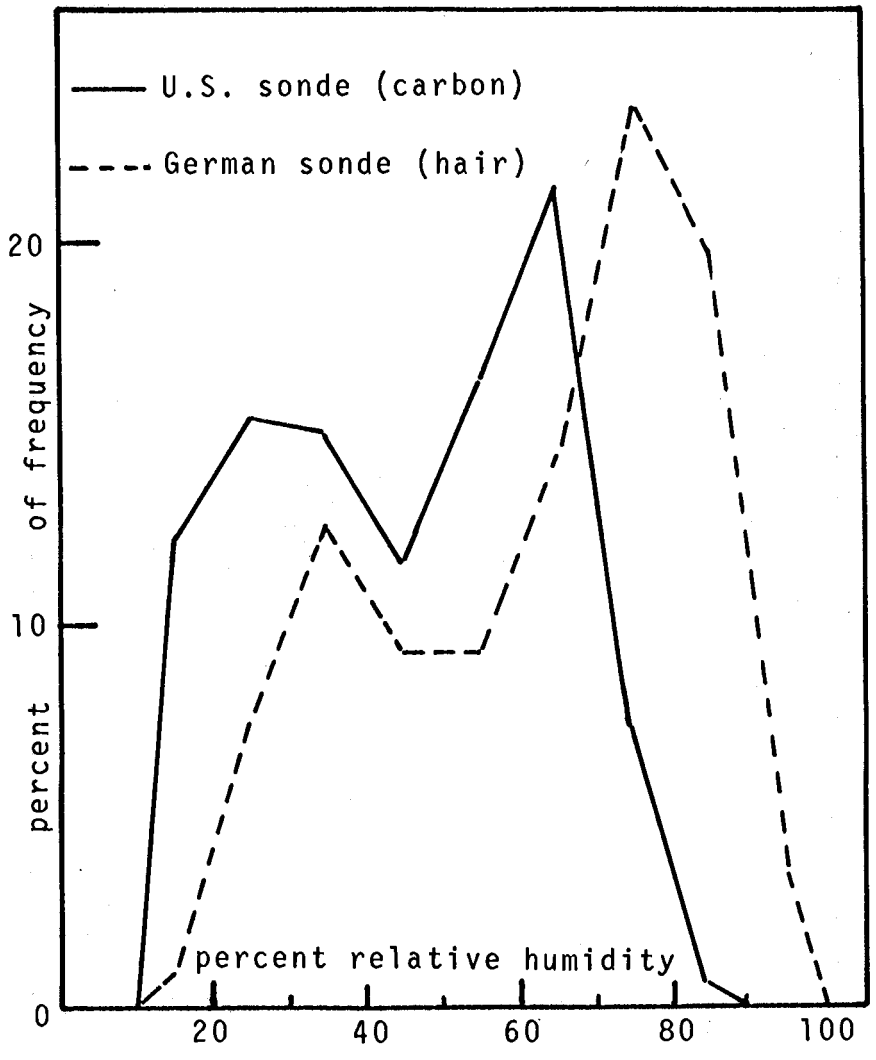

Figure 10. Daytime observations of relative humidity frequency distribution of the U.S. and German sonde.

above 0°C for the German M60 humidity recordings and the U.S. 403 MHz sonde. Figure 11 shows the same statistics for the night flights (2200 local time).

As seen from figure 10, only a few relative humidities above 80 percent were recorded with the U.S. sonde and the relative frequency maximum has shifted from 75 percent RH, as recorded by the hair hygristor, to 65 percent RH, as recorded by the carbon element. At night, distributions are similar, especially at high humidities. At low humidities the hair

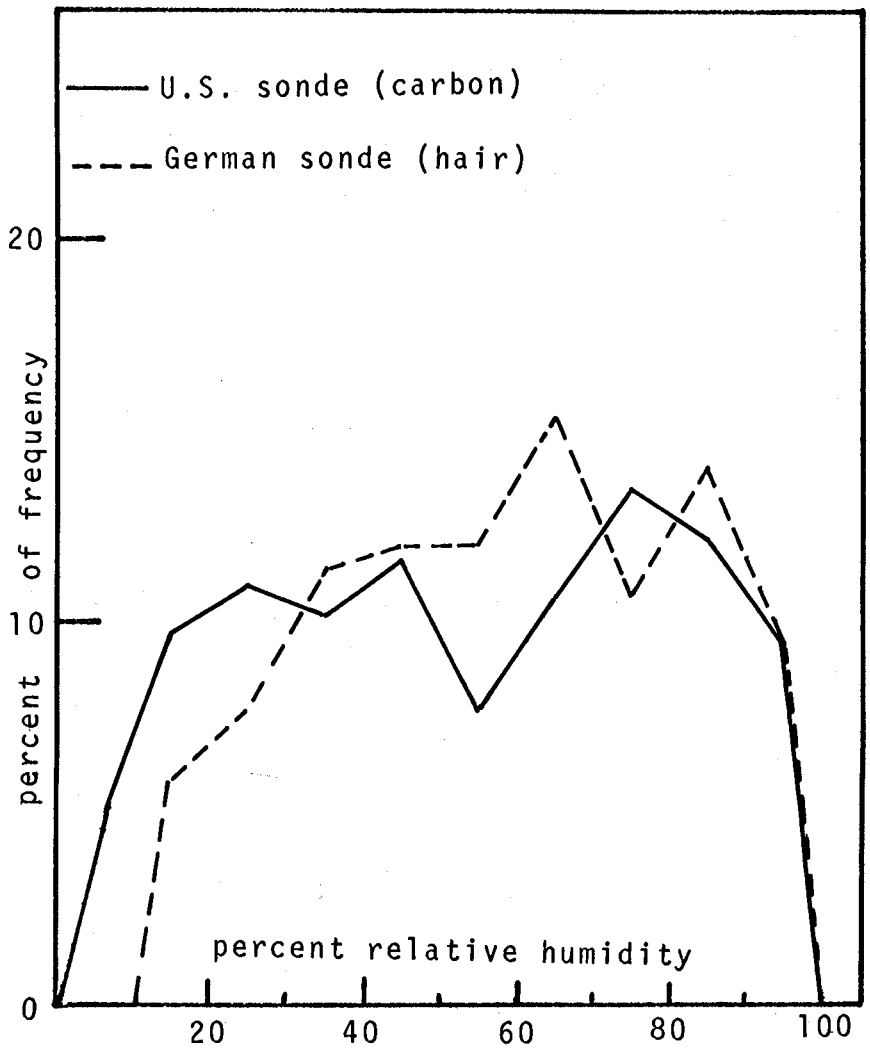

Figure 11. Relative humidity frequency distribution of U.S. and German sonde night observations.

hygristor values are lower at daytime as well as at nighttime. This may be due to the poorer response of the hair hygristor to lower humidities or the relatively long time constant of the carbon hygristor system due to poor ventilation (see sec. 3.2) or both.

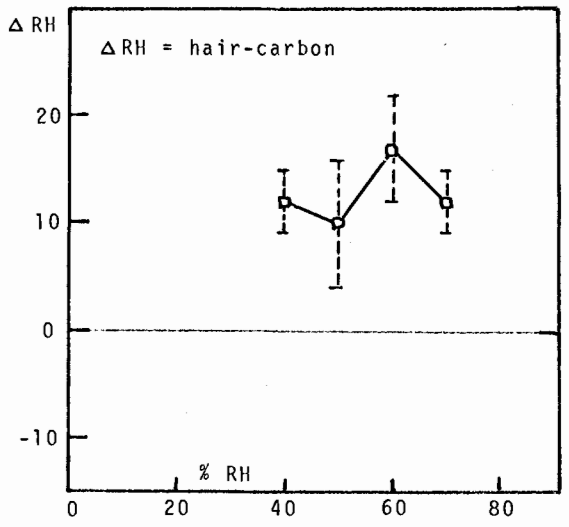

Figure 12. Frequency of occurence of difference between carbon and hair RH for day observations.

The difference in RH between the hair hygristor readings minus the carbon element readings was plotted against the reported humidity from the carbon element, both for the daytime ascents (fig. 12) and the nighttime ascents (fig. 13). The vertical bars indicate the standard deviation. Although there were not nearly enough cases for the nighttime values, the results as shown in figure 13 support the assumption that little error is present in the nighttime ascents. Therefore, no attempt was made to correct the nighttime readings.

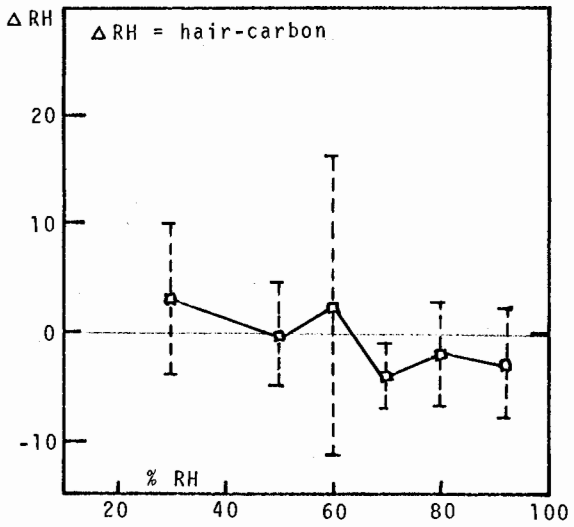

Figure 13. Frequency of occurence of difference between carbon and hair RH for night observations.

The Meteorological Institute of the University of Hamburg (Prof. K. Brocks, Director) developed a special sonde that is used for flights up to about 21,000 feet. The sonde consists of a vertical aluminum tube (2 inches x 2 inches x 12 inches) containing a dry thermistor

bead, wet thermistor bead, and the carbon hygristor. The altitude is determined by radar tracking. These sondes were used during ATEX on the German R/V *Meteor* and *Planet*. The RH as recorded by the carbon hygristor and as derived from the dry- and wet-bulb temperatures were similar. This is further evidence that the solar radiation contributes most to the daytime humidity errors on the U. S. 403 MHz sonde.

5. ATEX DATA CORRECTIONS

All daytime radiosonde ascents that were made from *Discoverer*, *Meteor*, *Planet*, and *Hydra* during ATEX with the U. S. 403 MHz radiosonde will be corrected according to amounts presented in figure 14. Curve 1 was derived from the comparison flights from the *Meteor* (sec. 4). Independently, curve 2 was constructed from the comparison flights in Miami (sec. 2.2). In figure 14 the deficiency in RH, ΔRH, is plotted

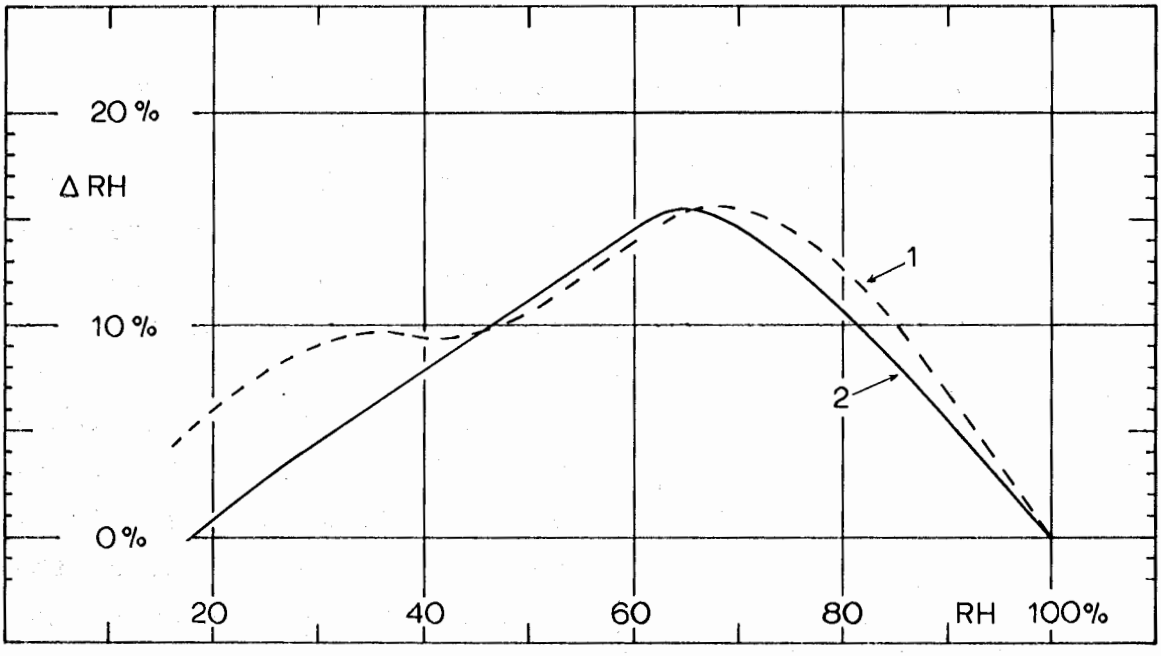

Figure 14. Correction curves for carbon hygristor due to solar heating. Curve 1, based on the German hair hygrometer, includes data for temperatures below 0°C. Curve 2, based on SAIL's modified radiosonde, is for temperatures above 0°C.

against the RH reported by the regular 403 MHz sonde. These data were obtained under clear sky conditions with a few small trade wind cumuli, a good simulation of the general weather conditions during ATEX.

An example may illustrate the application of the graph. If the regular 403 MHz sonde reports, say, 80 percent RH, then to this value RH = 11 percent is added to give 91 percent RH. For 70 percent RH reported, the corrected value reads 85 percent, etc. Test calculations showed, however, that at very low altitudes (up to about 995 mb) this correction leads to over estimates.

During the baseline check of the modified and regular radiosonde, each was exposed to the same humidity conditions and calibrations were adjusted to show this. Upon release and exposure to solar heating, the transmitted humidity values diverged such that after about 40 sec the solar heating effect stabilized. This level averaged out near 200 m or 995 mb for the test data. A family of curves similar in shape to curve 2 in figure 14, but with decreasing amplitude from 200 m to the surface, has been developed to correct values during the period of divergence due to initial heating.

It should be emphasized most emphatically that these corrections may be applied confidently only for the conditions comparable with those under which they were derived, namely, the undisturbed trade wind conditions as prevalent on ATEX. To verify the validity of the correction curve, we plotted the 32 day and 32 nighttime radiosonde observations made in the subtropical Atlantic during July and August. As shown in figure 15, corrections were applied to the daytime humidity values and the resulting curve matched the nighttime values quite closely.

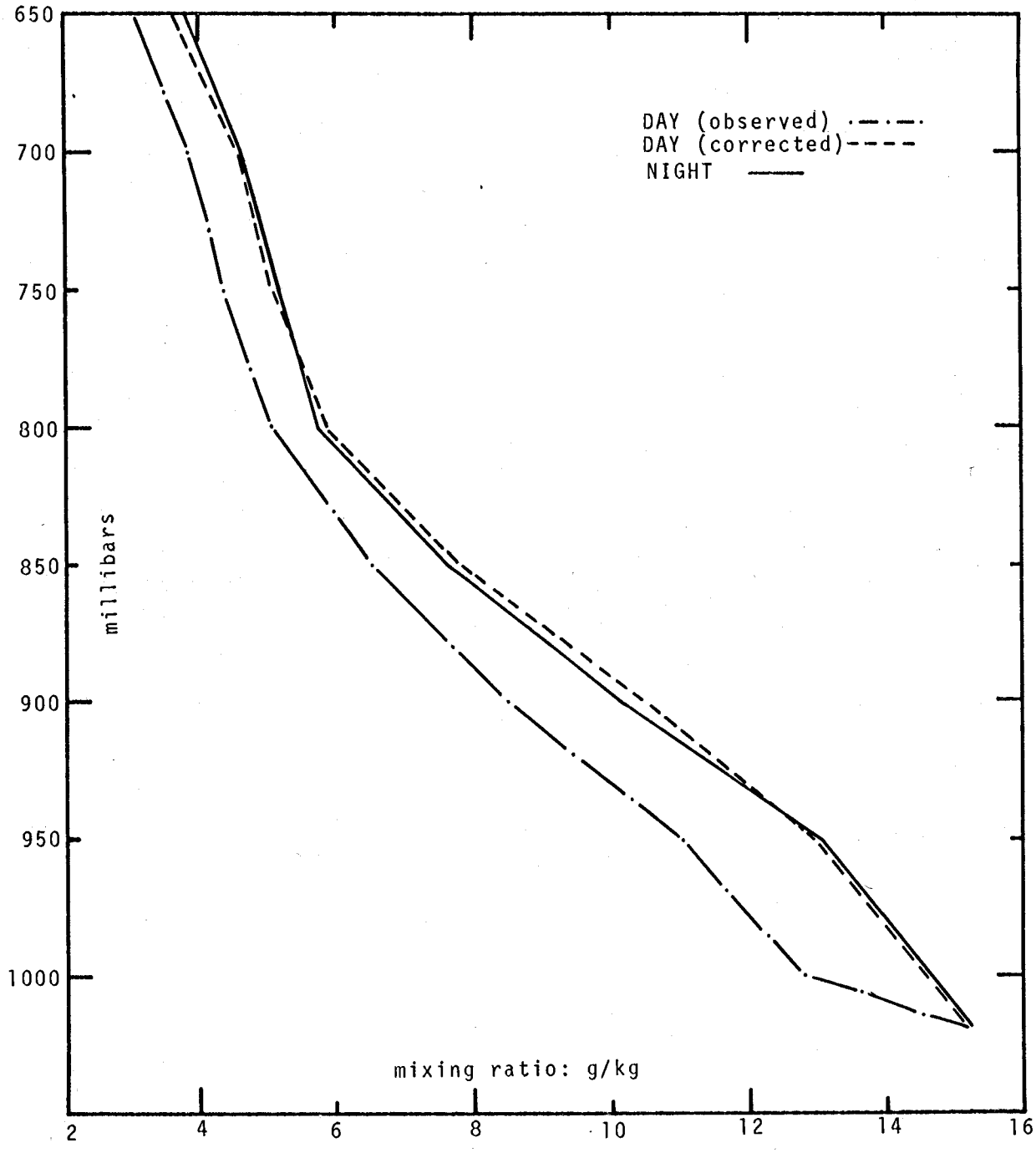

Figure 15. Data for 32 day and 32 night radiosonde observations made during July and August 1970 in the Atlantic.

6. CONCLUSION

The relative humidities obtained by the U.S. radiosonde with the carbon element humidity sensor may indicate values that are incorrect by a substantial amount. The principal reason for this error is the temperature of the element itself. If the element for any reason operates on a higher (or lower) temperature level than the environmental temperature, the air over the surface of the element will be heated (or cooled); therefore, the saturation water vapor pressure will be raised (or lowered), resulting in a lower (or higher) RH.

The carbon element may acquire a different temperature than the environmental temperature during the daytime, principly because of radiative heating. A second source of error is the heat capacity of the carbon element itself, which leads to a temperature lag while the radiosonde is rising through the atmosphere. With an adiabatic lapse rate this process will also tend to indicate humidities that are too low. In an inversion the result is opposite.

Considerable improvement could be achieved by changing the exposure of the carbon element to provide a radiation shield and better ventilation.

7. ACKNOWLEDGEMENTS

We express our appreciation to Mr. O. Scribner of the Field Research Projects Office for calling our attention to the problem and Dr. A. Glaser of BOMAP for suggestions regarding the study. Although all of the Sea Air Interaction Laboratory staff were involved in the study, particular thanks are due Messrs. D. Waters, M. Poindexter, P. Connors, and Dr. W. McLeish for their contributions. We are grateful to Dr. C. Pflugbeil of the Deutscher Wetterdienst Seewetteramt at Hamburg (German Marine Weather Office) for generously providing the *Meteor* data used in this study.

8. REFERENCES

Marchgraber, R. M., and H. H. Grote (1965), The dynamic behavior of the carbon humidity element ML-476. Humidity and Moisture I (Reinhold Publishing Corporation, New York, N. Y.).

Morrissey, J. F., and F. J. Brousaides (1970), Temperature induced errors in the ML-476 humidity data, J. of Applied Meteorology 9, No. 5, 805-808.

Muller, H. G. (1965), Humidity sensors from natural materials, Humidity and Moisture I (Reinhold Publishing Corporation, New York, N. Y.).

APPENDIX A

Radiosonde Temperature and Humidity Data

The following 50 figures illustrate the data gathered during these experiments at Miami. Both the modified and unmodified sondes are included. The results of the first ascent are shown in figures A1 (relative humidity) and A2 (temperature). Figure A5 is a comparison of the alu-modification with the vertical duct type modification. Figure A11 is an example of typical trade wind conditions; figures A23 and A24 show data taken during thick overcast conditions. Figures A35 through A50 also show relative humidity measured at exactly the same time by each pair of sondes.

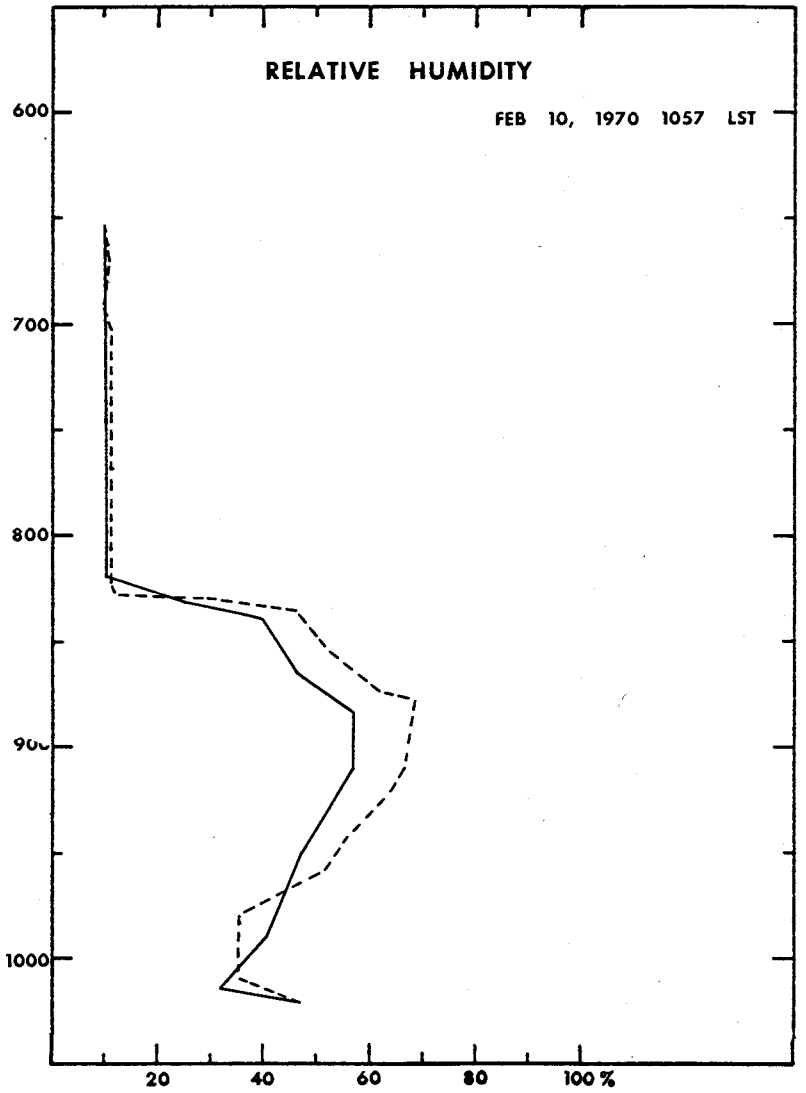

Figure A1. Standard sonde trace —— alu-modification -----.

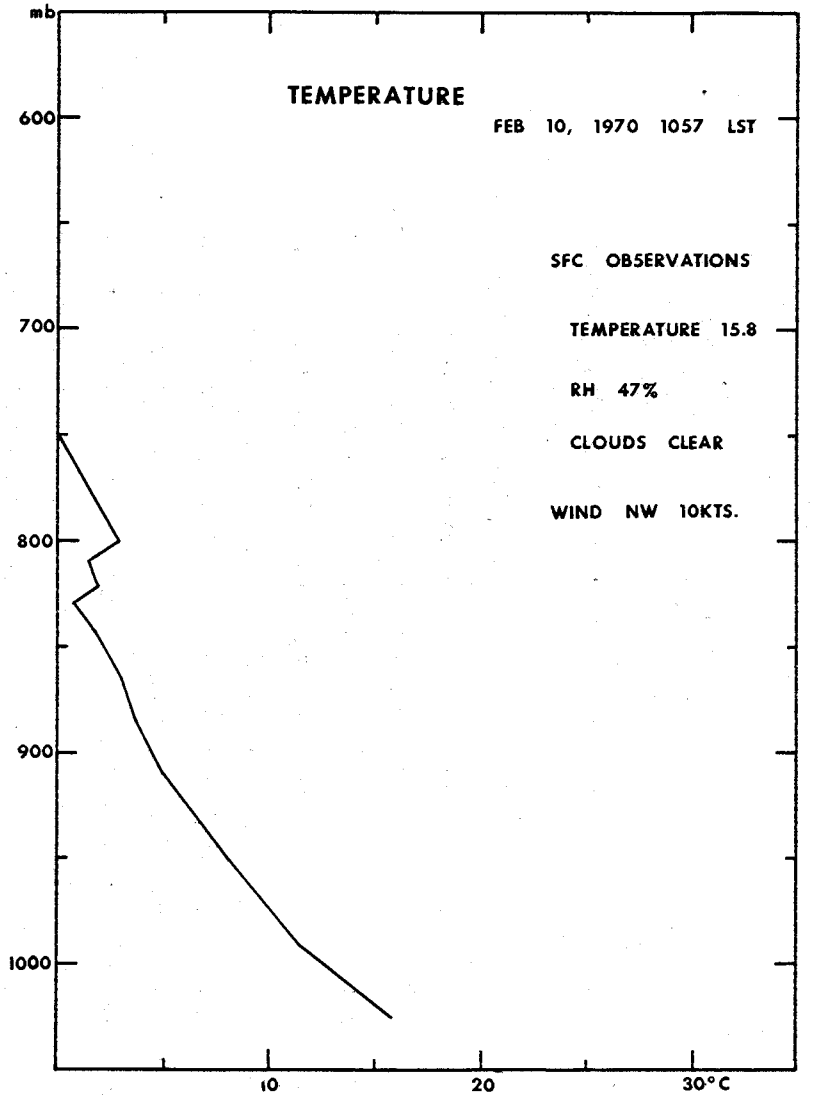

Figure A2. Standard sonde temperature curve.

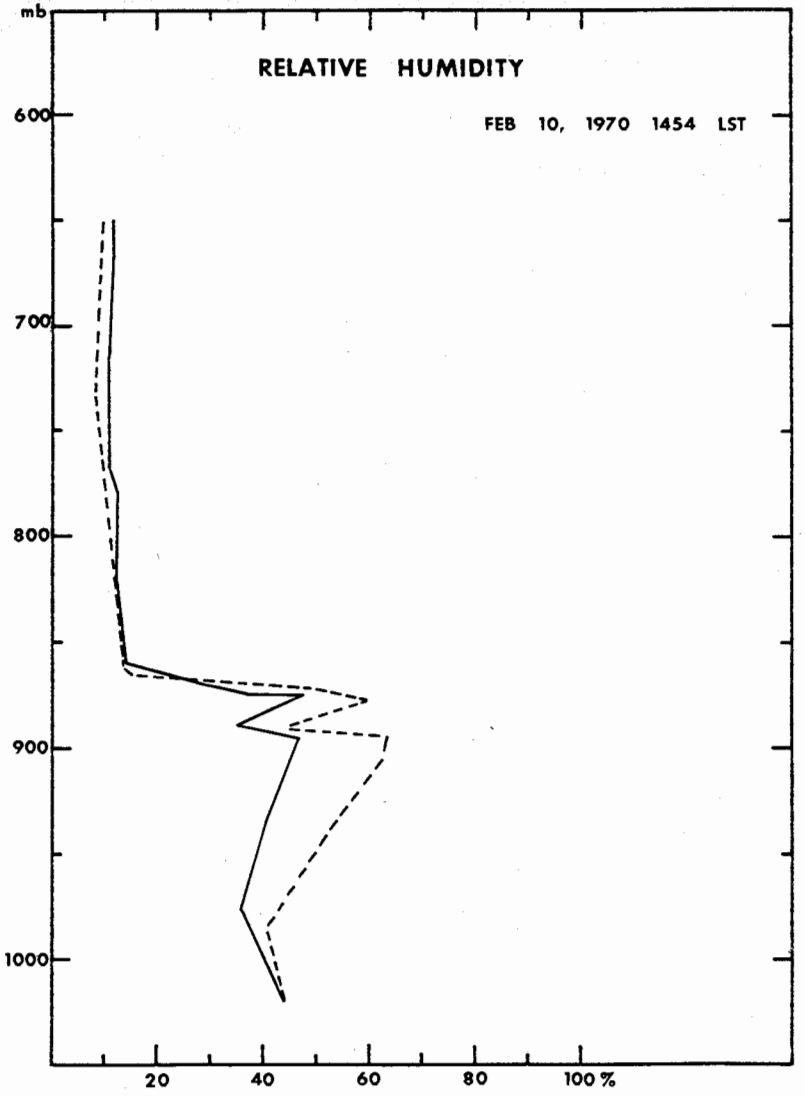

Figure A3. Standard sonde trace ——— vertical tube modification -----.

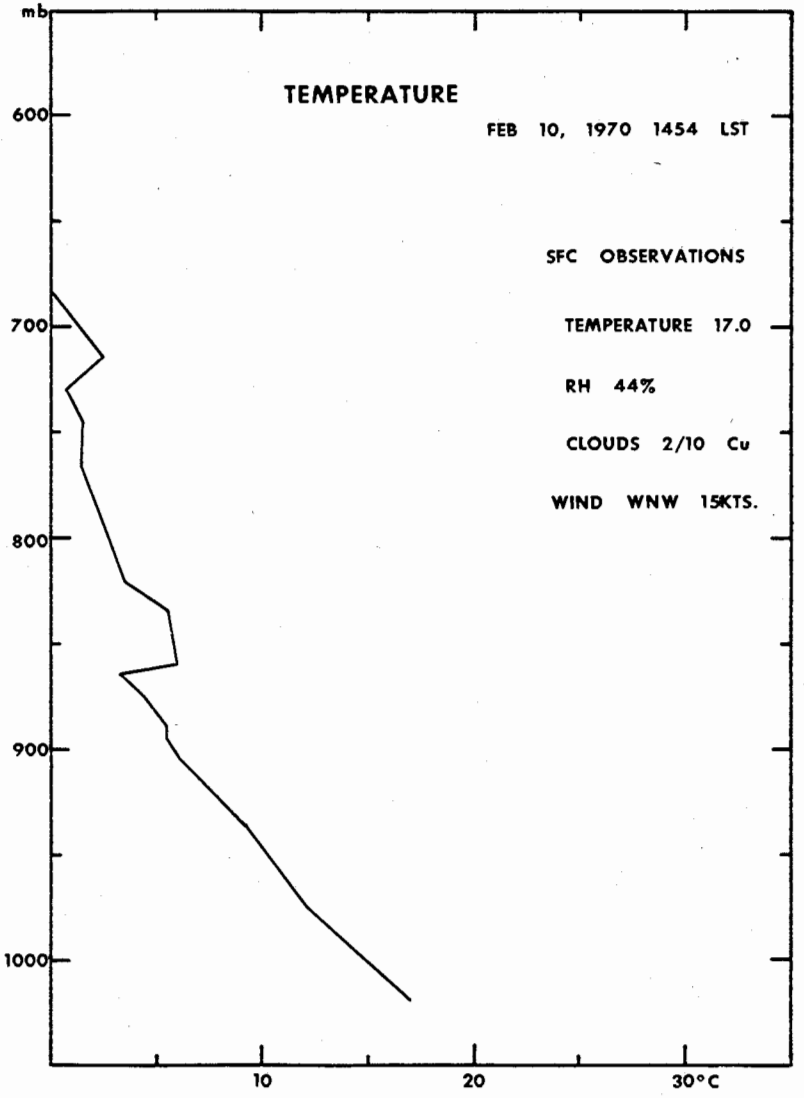

Figure A4. Standard sonde temperature curve.

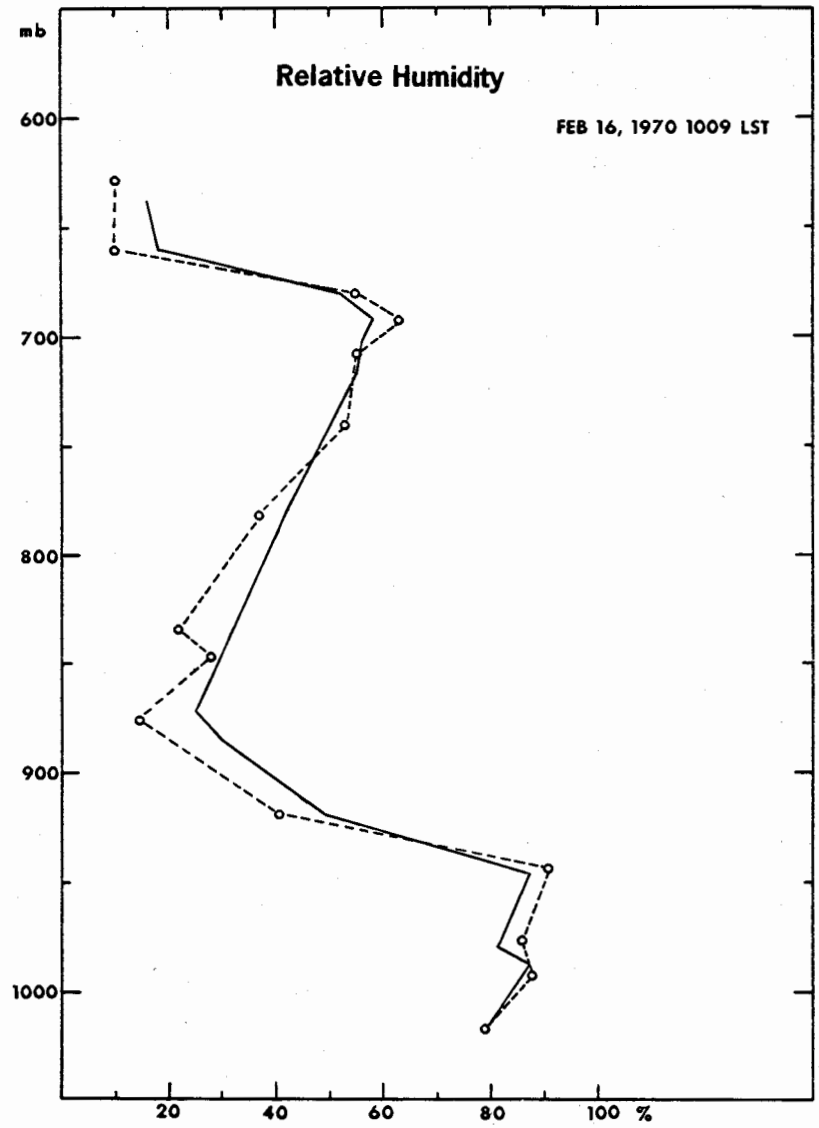

Figure A5. Alu-modification ——— vertical tube -----.

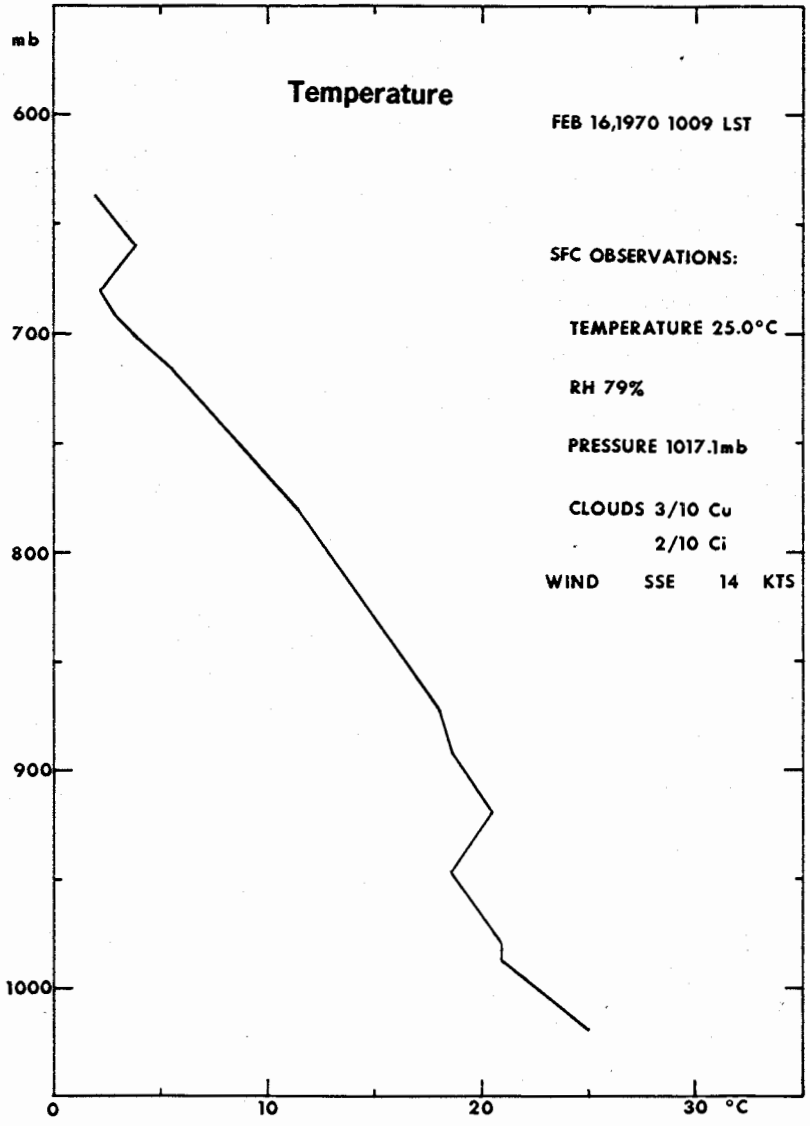

Figure A6. Temperature curve for aluminum foil modification.

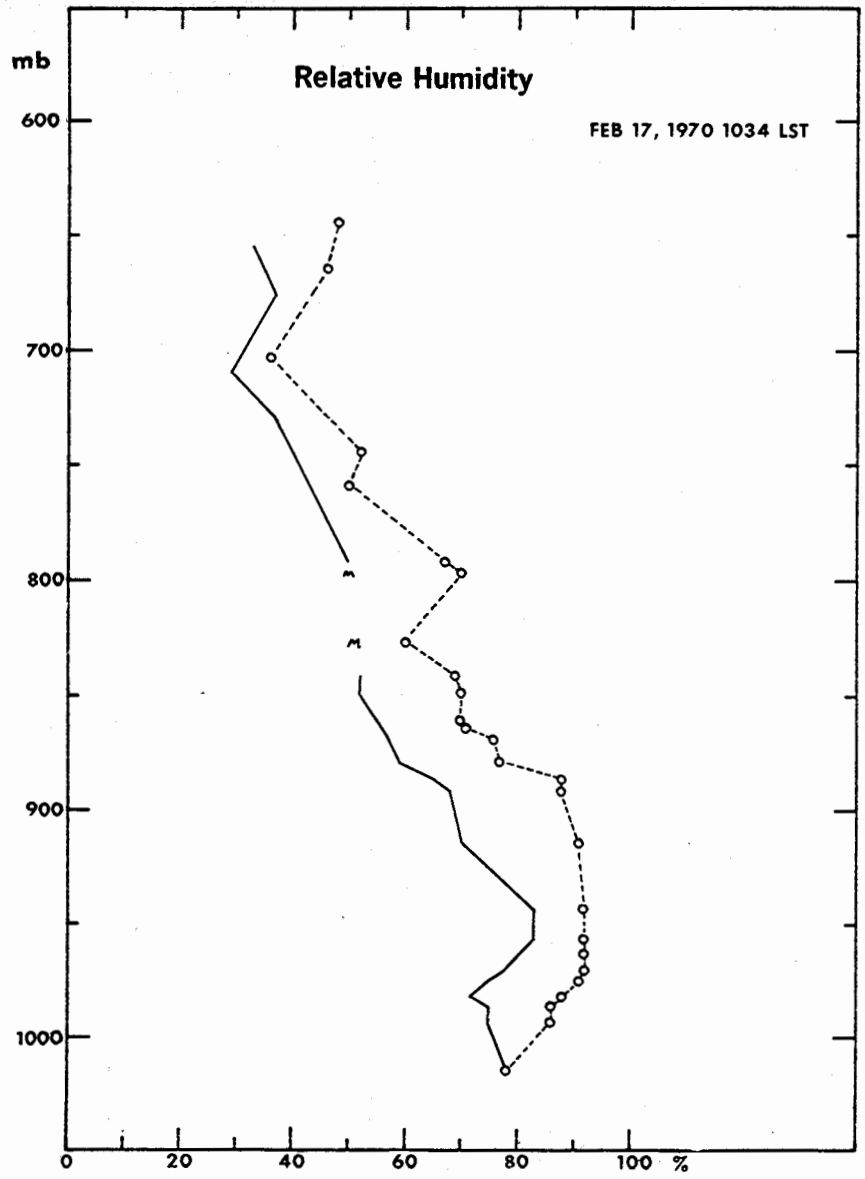

Figure A7. Standard sonde ——— vertical tube -----.

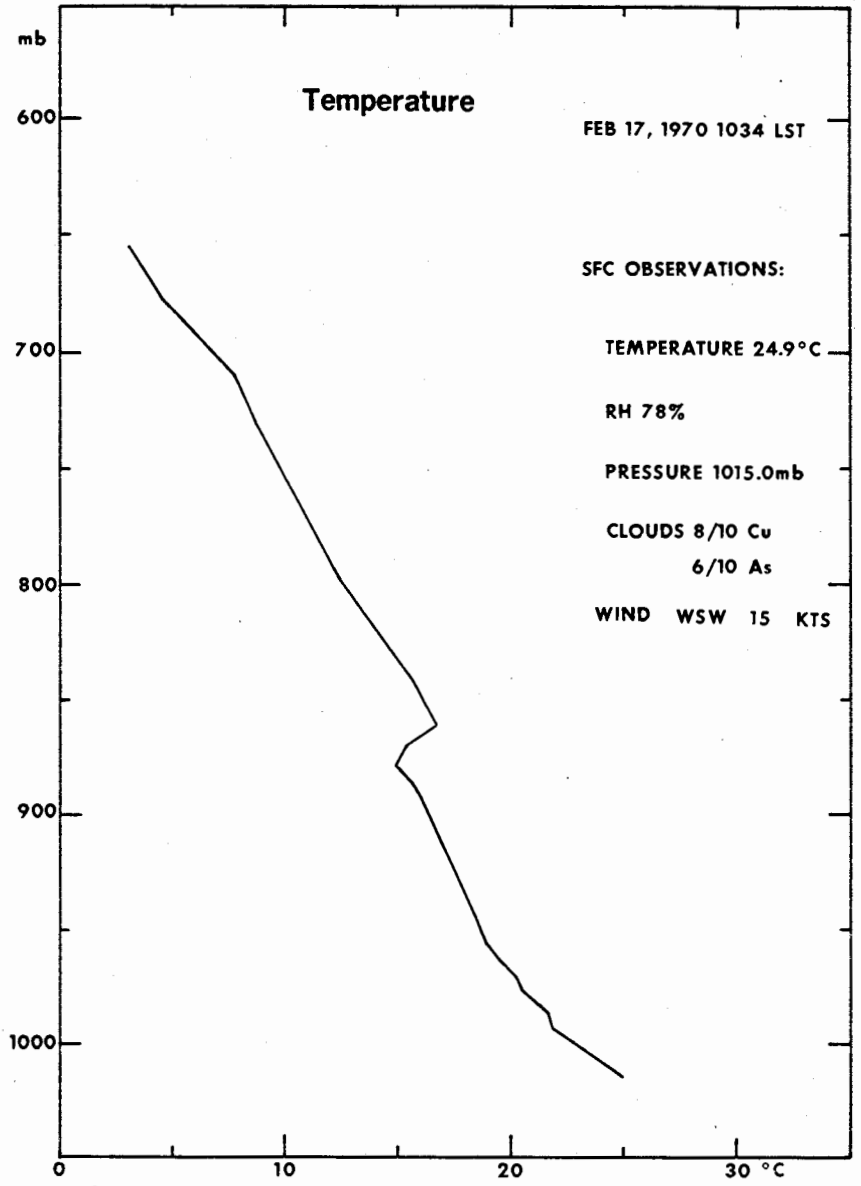

Figure A8. Standard sonde temperature curve.

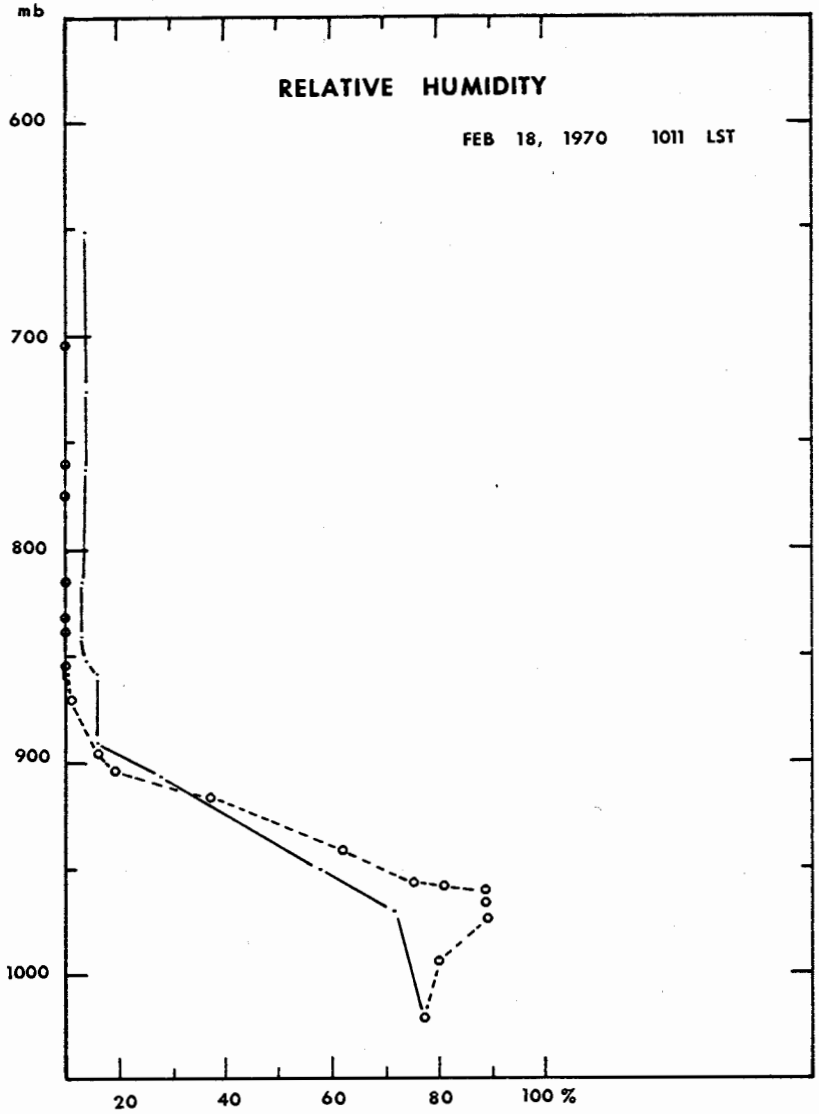

Figure A9. Standard sonde ——— vertical tube -----.

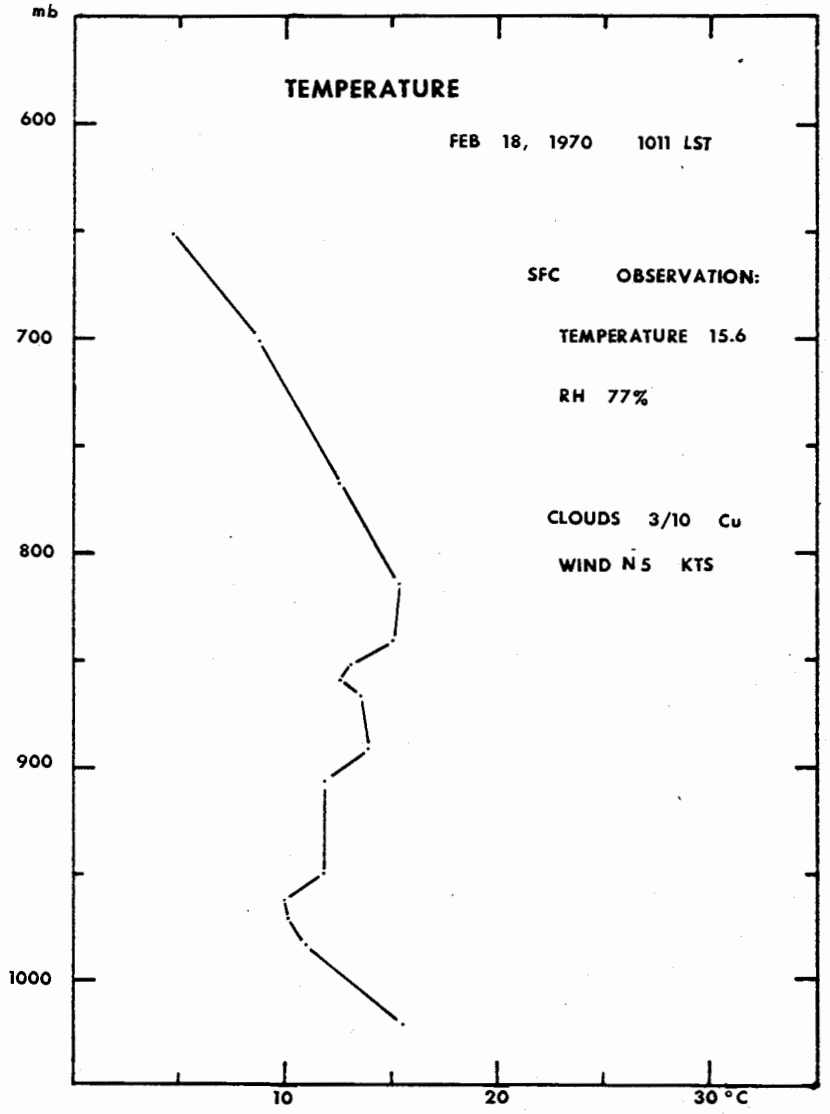

Figure A10. Standard sonde temperature curve.

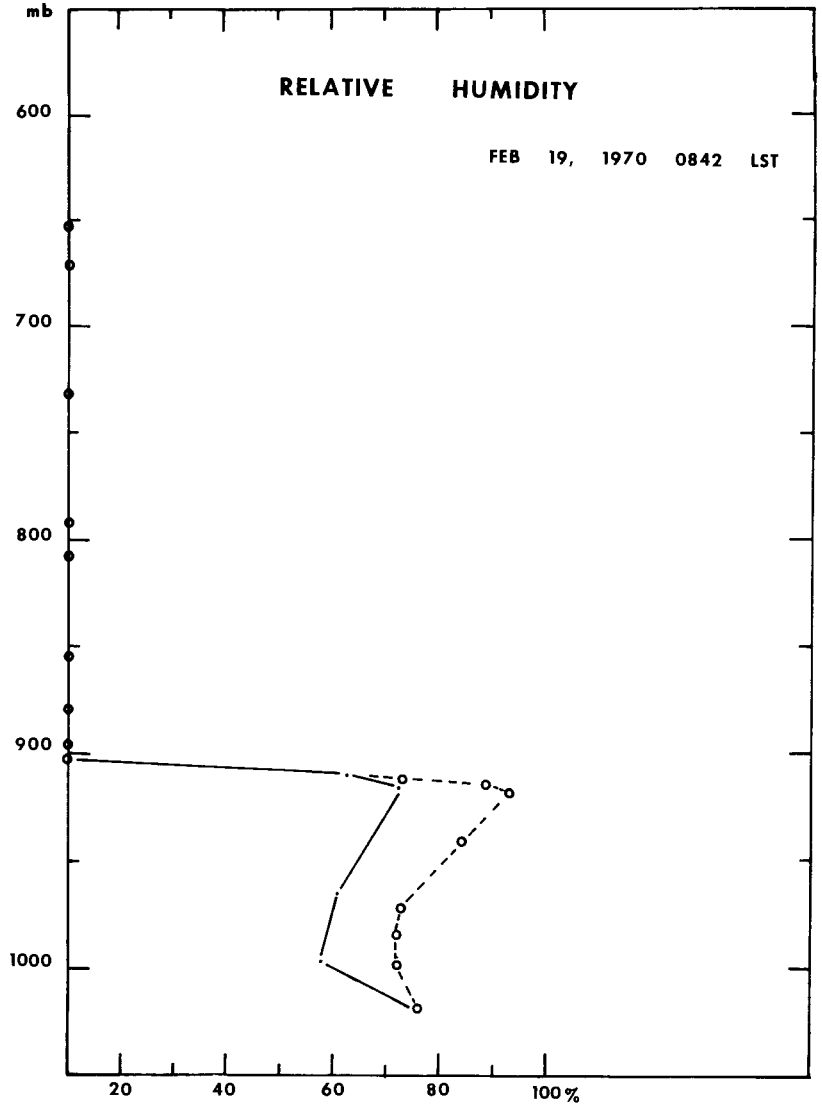

Figure A11. Standard sonde ——— vertical tube -----.

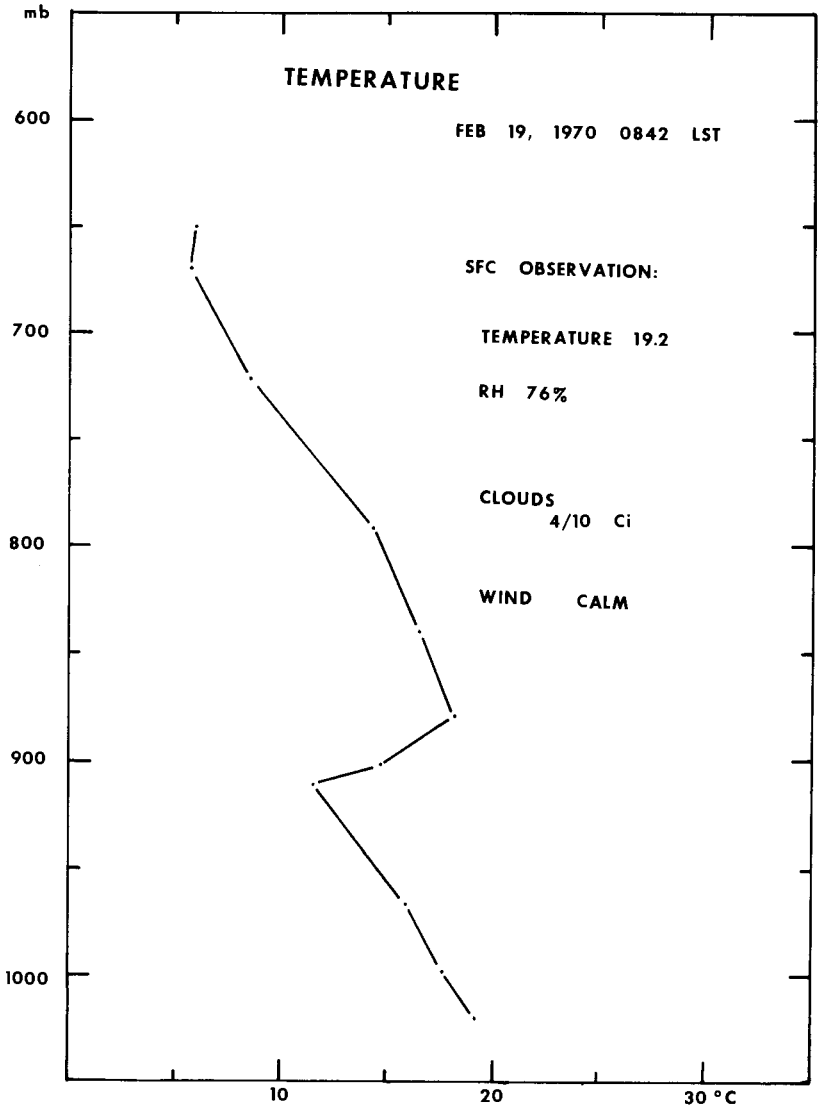

Figure A12. Standard sonde temperature curve.

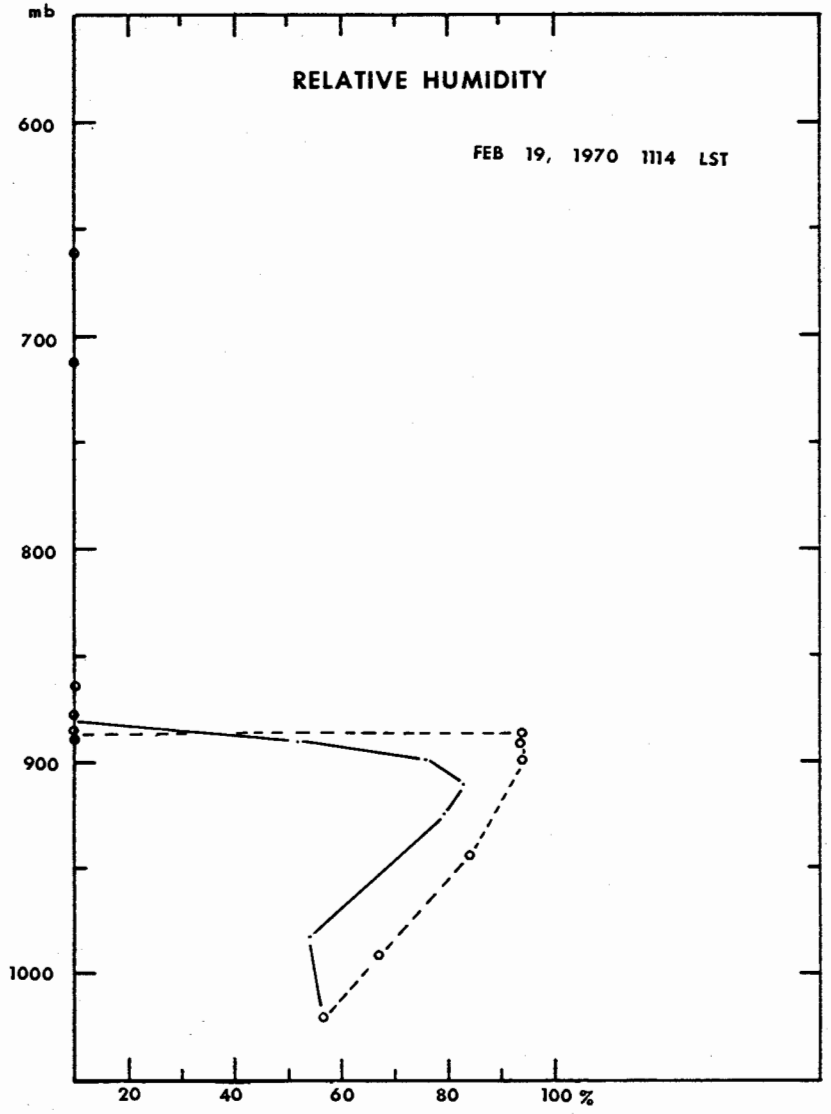

Figure A13. Standard sonde —— vertical tube with a single precipitation baffle ----.

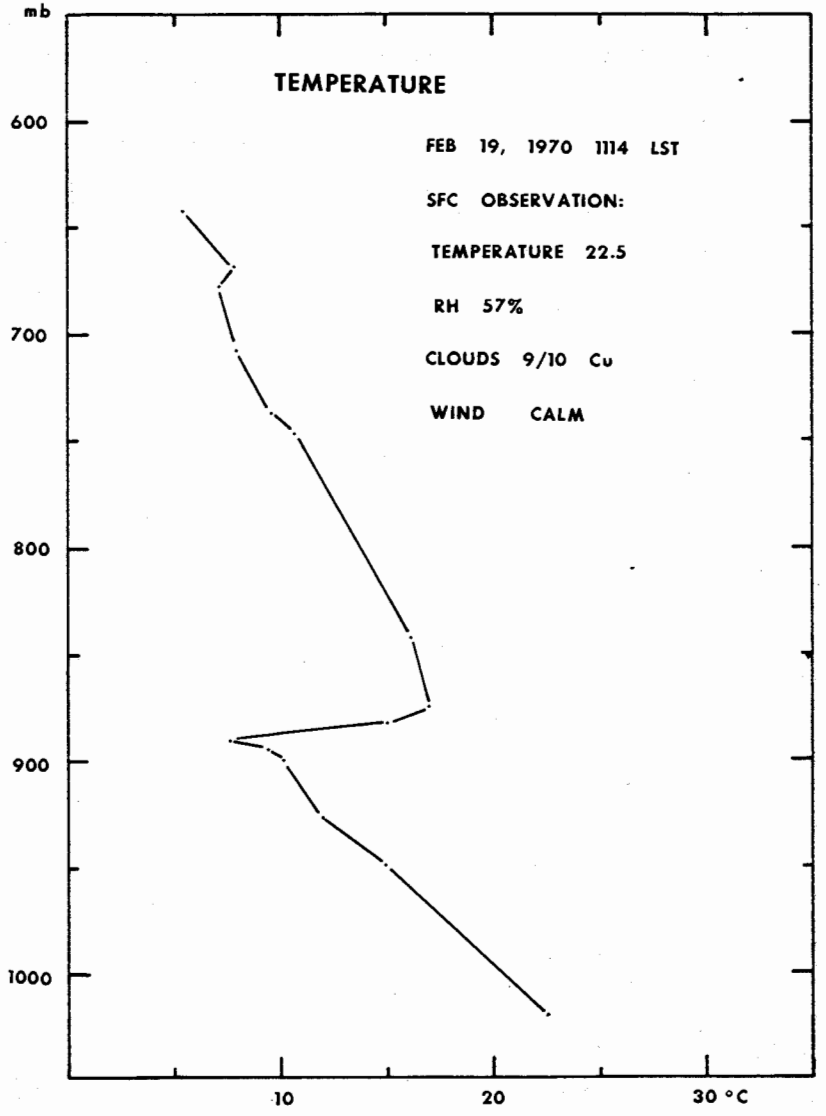

Figure A14. Standard sonde temperature curve.

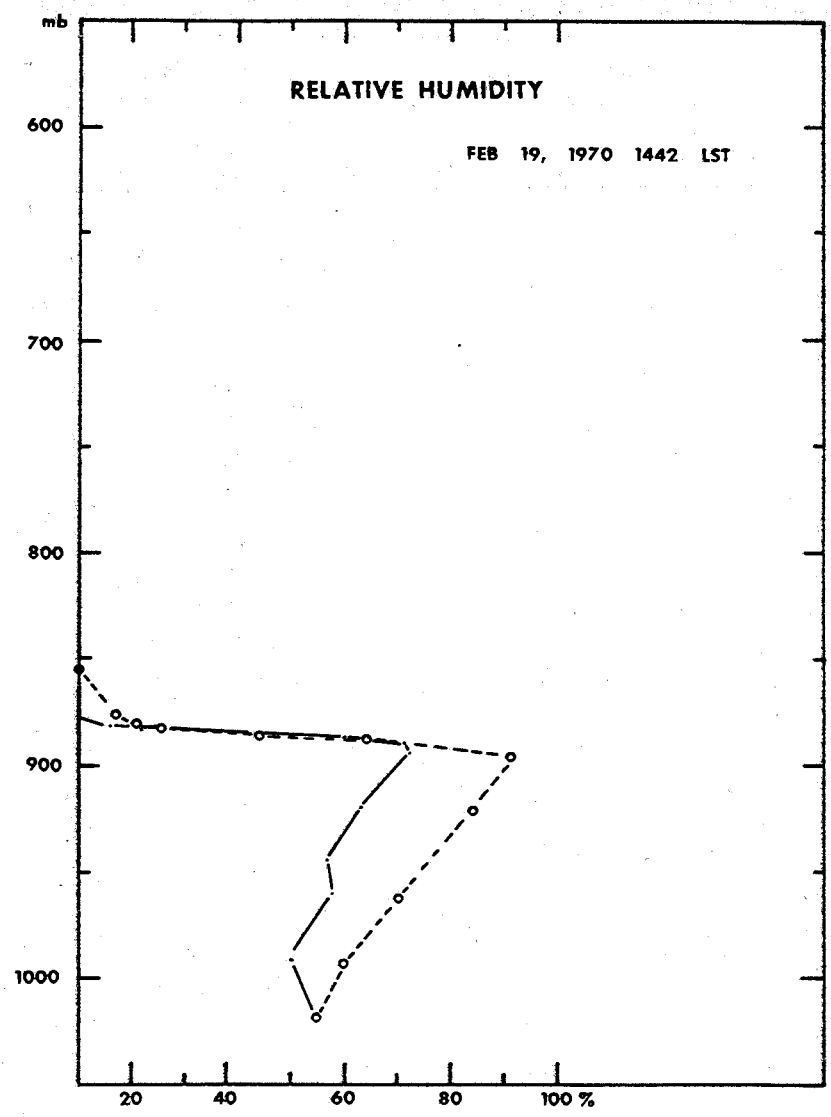

Figure A15. Standard sonde ——— vertical tube -----.

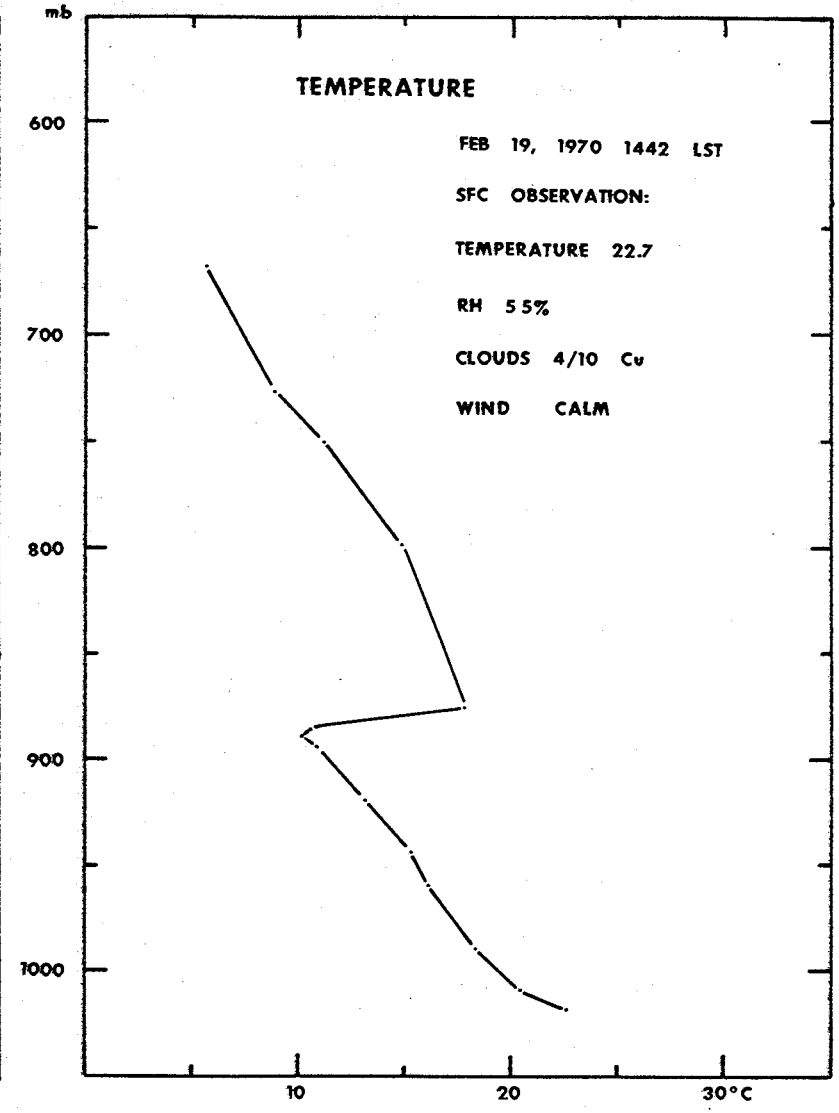

Figure A16. Standard sonde temperature curve.

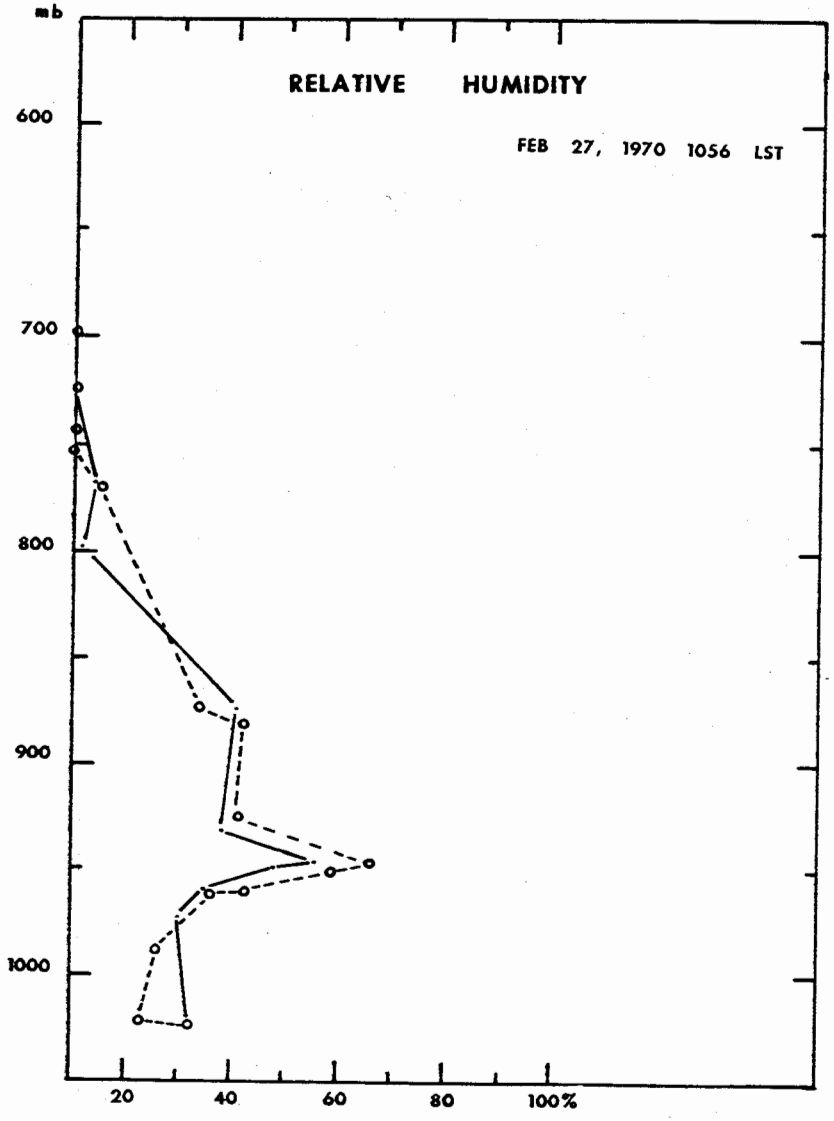

Figure A17. Standard sonde ——— alu- modification with ½ inch spacer be- low hygristor duct -----.

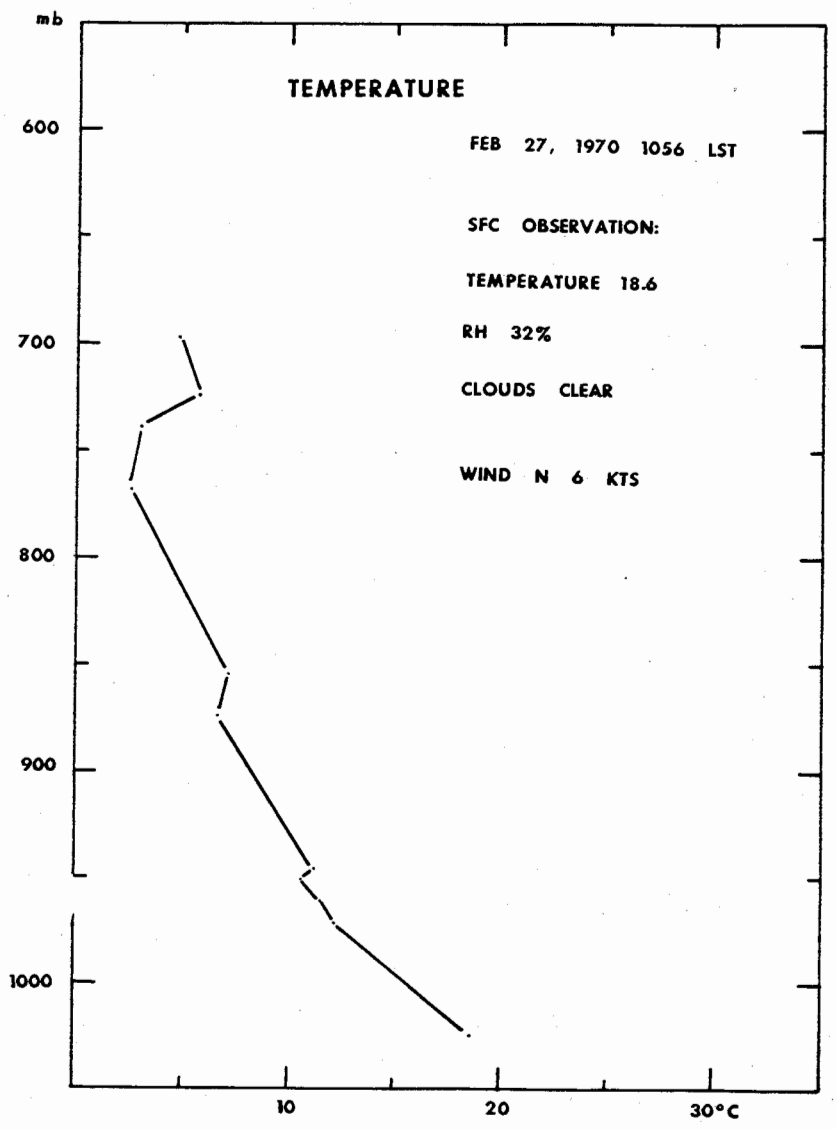

Figure A18. Standard sonde temperature curve.

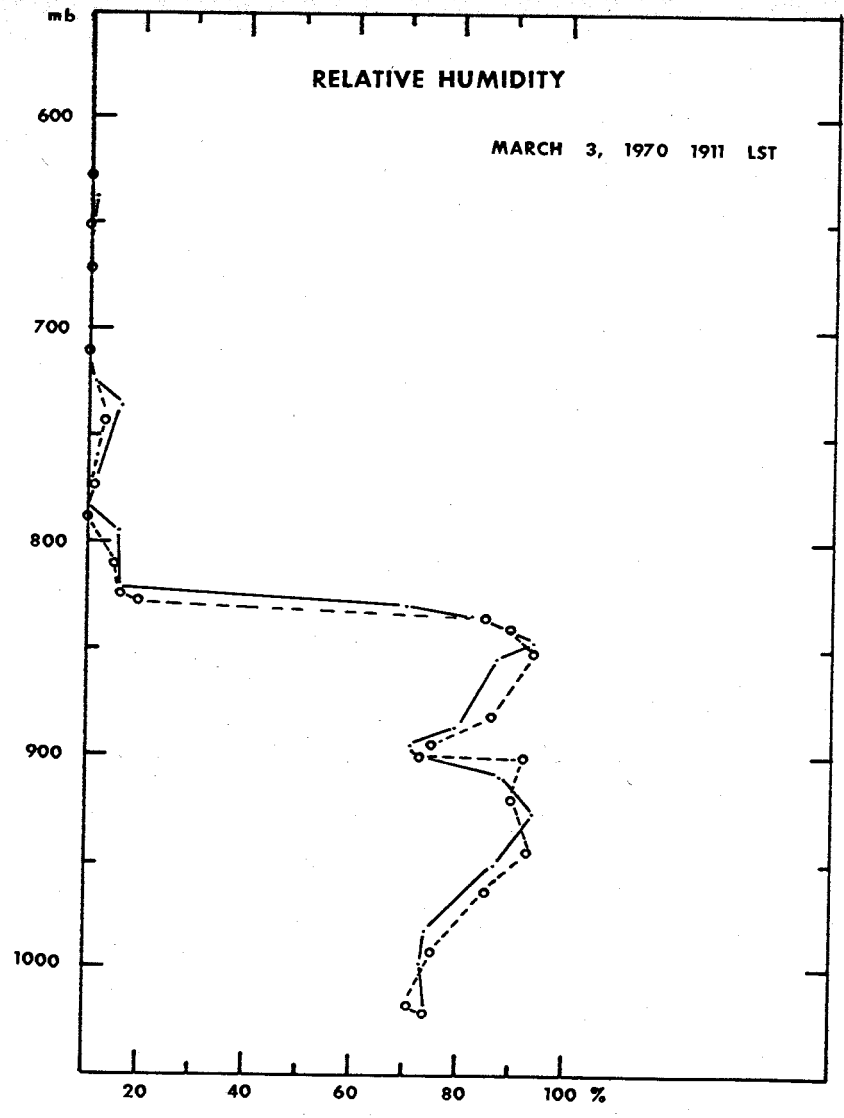

Figure A19. Standard sonde —— vertical tube -----.

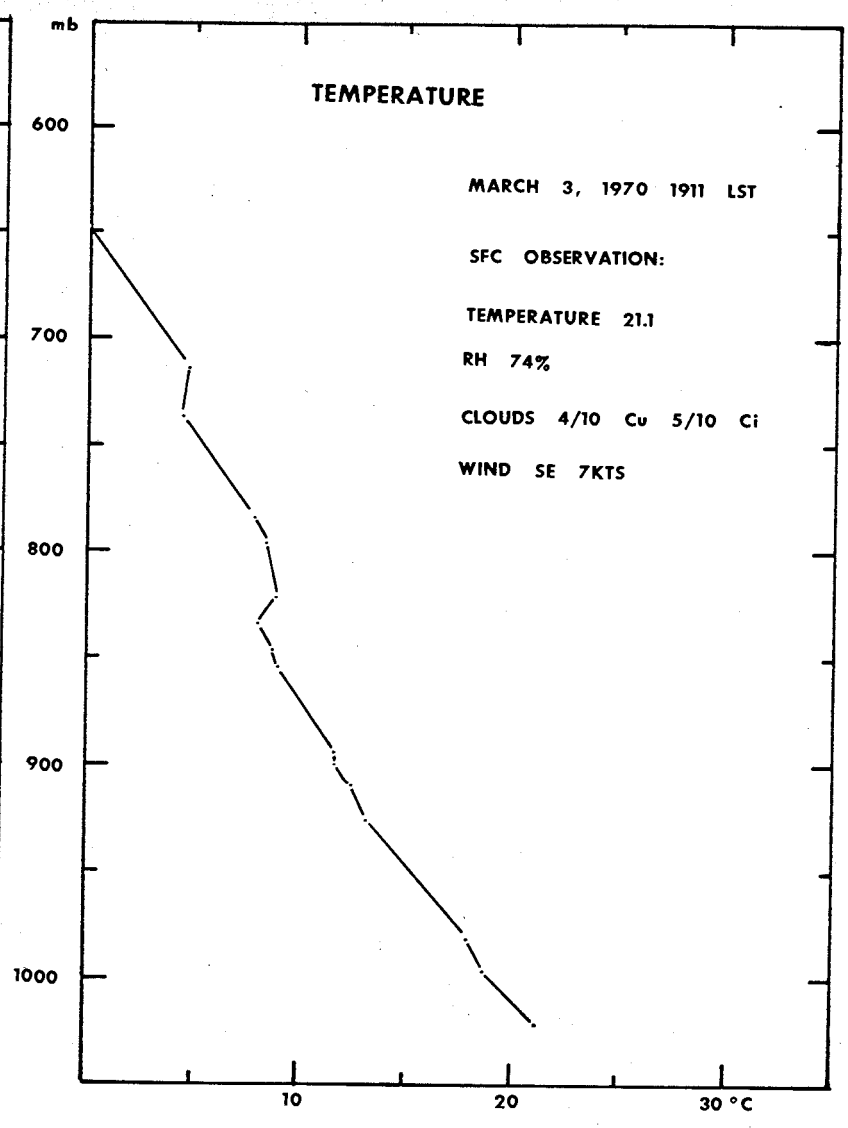

Figure A20. Standard sonde temperature curve.

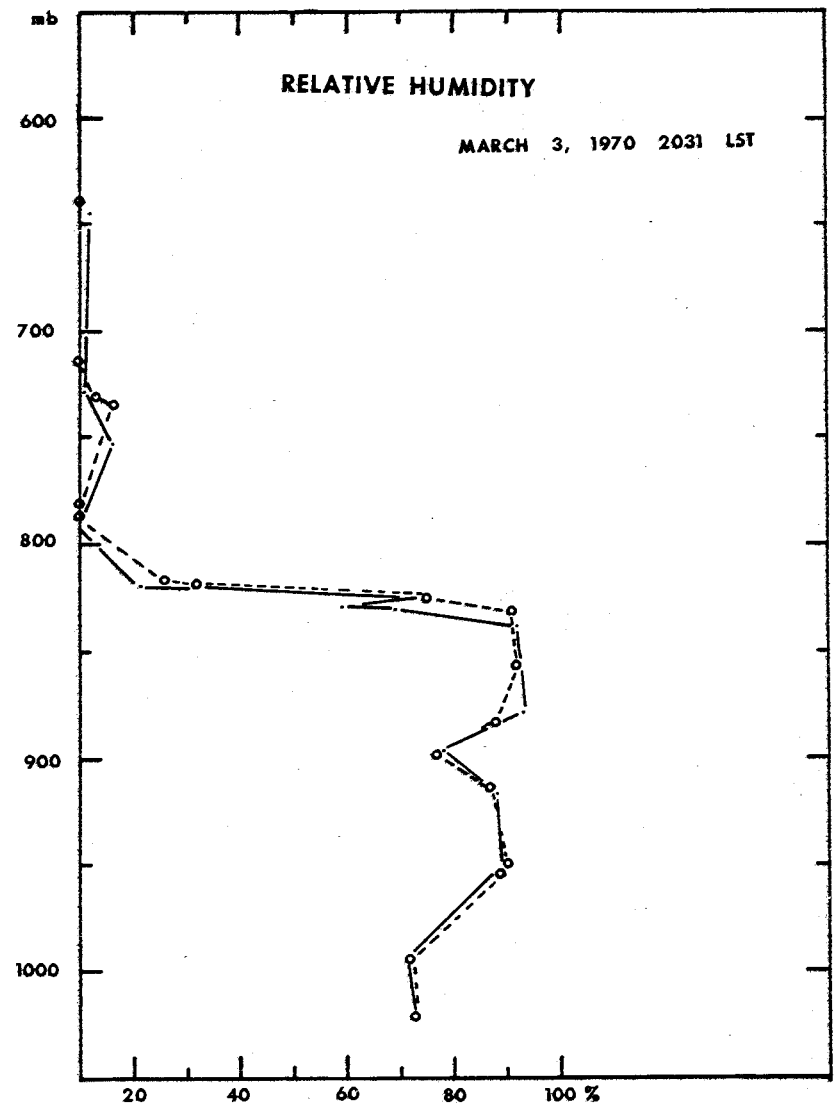

Figure A21. Standard sonde ——— vertical tube -----.

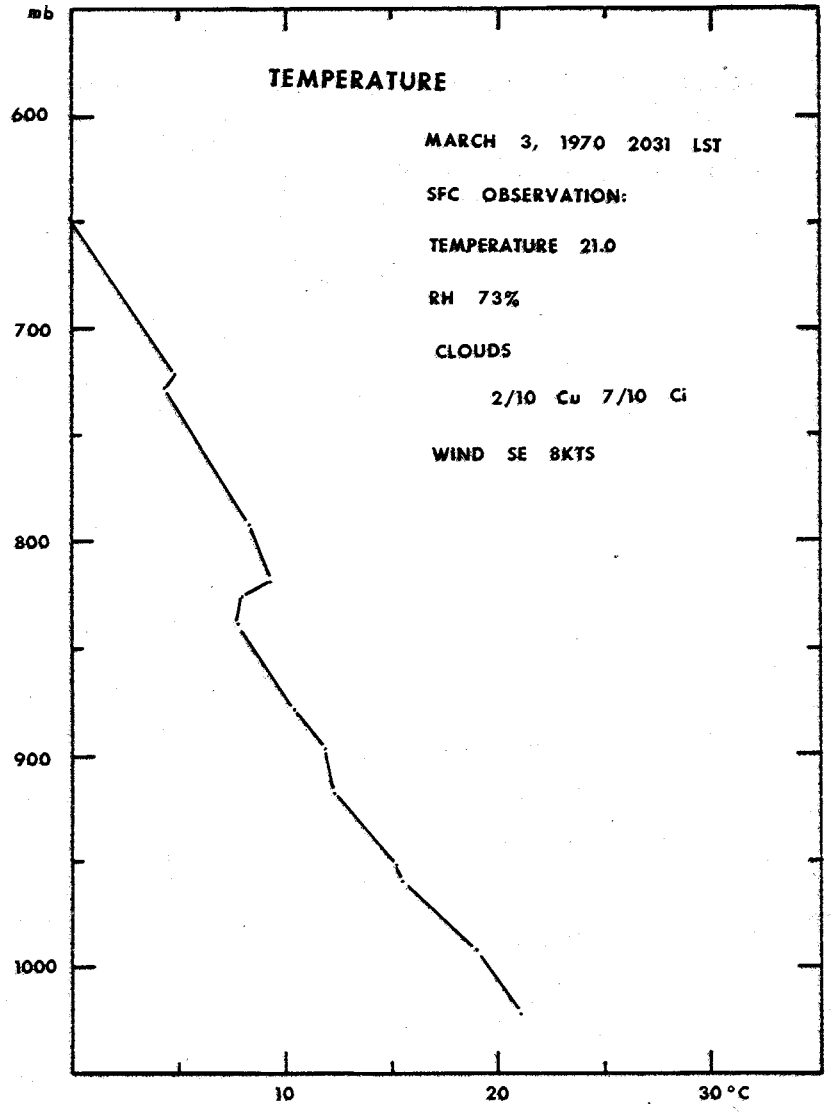

Figure A22. Standard sonde temperature curve.

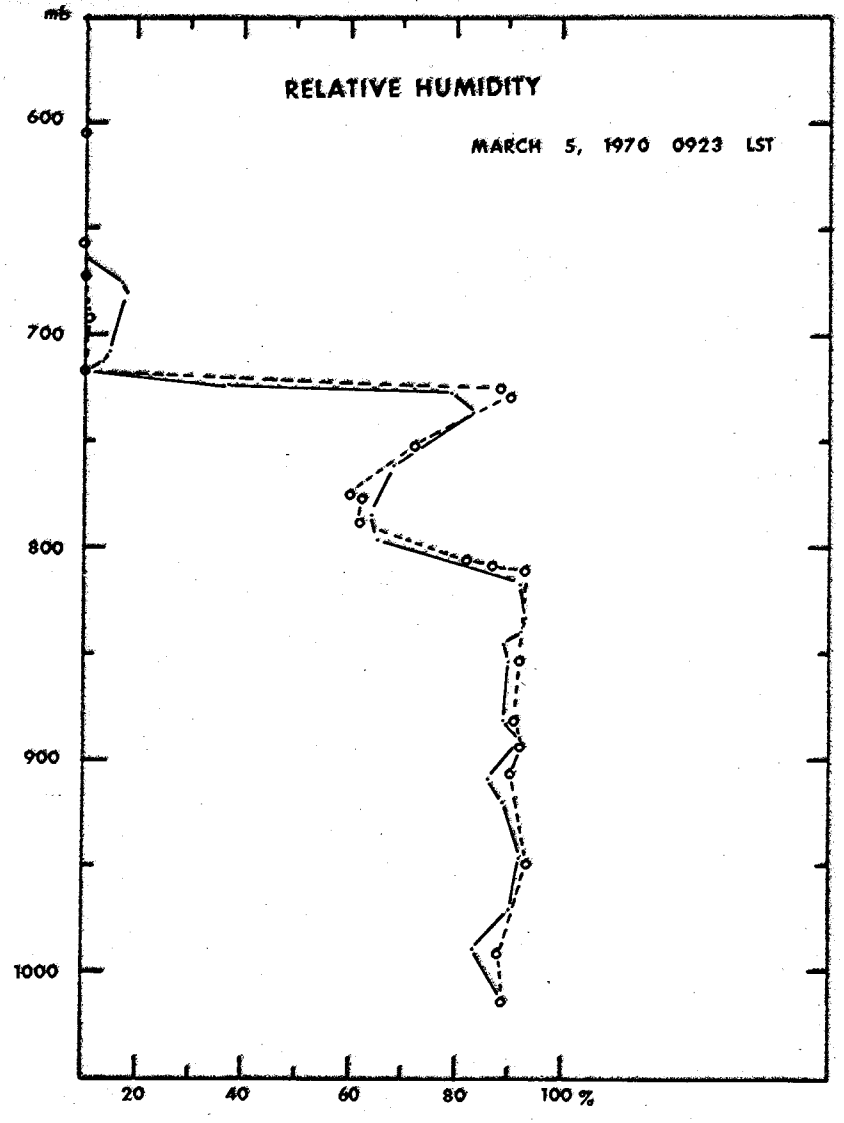

Figure A23. Standard sonde ——— vertical tube -----.

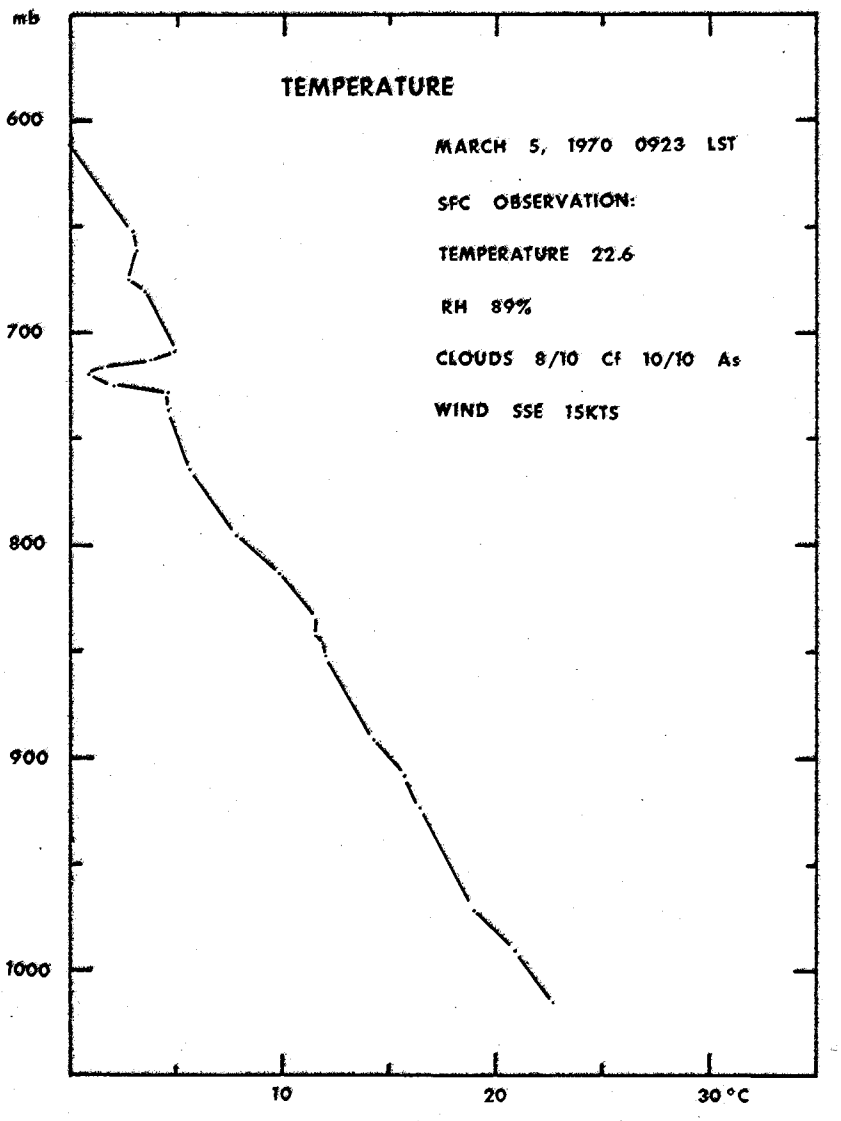

Figure A24. Standard sonde temperature curve.

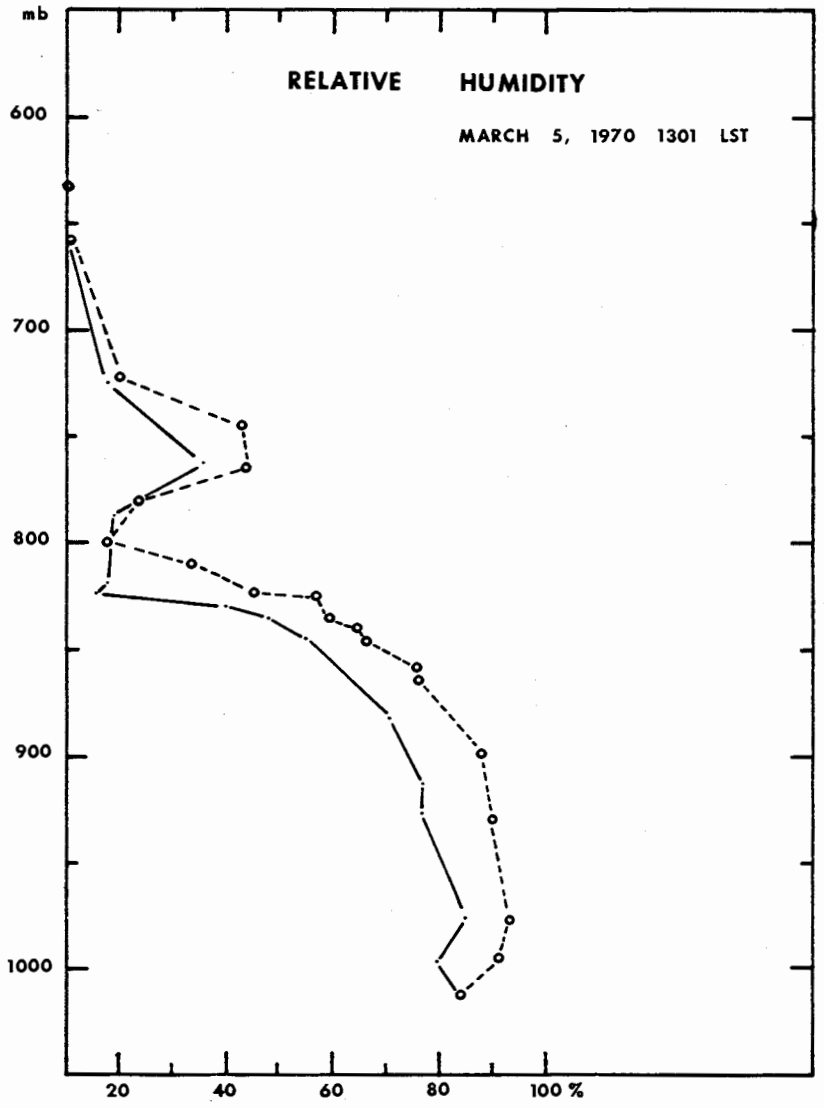

Figure A25. Standard sonde ——— vertical tube -----.

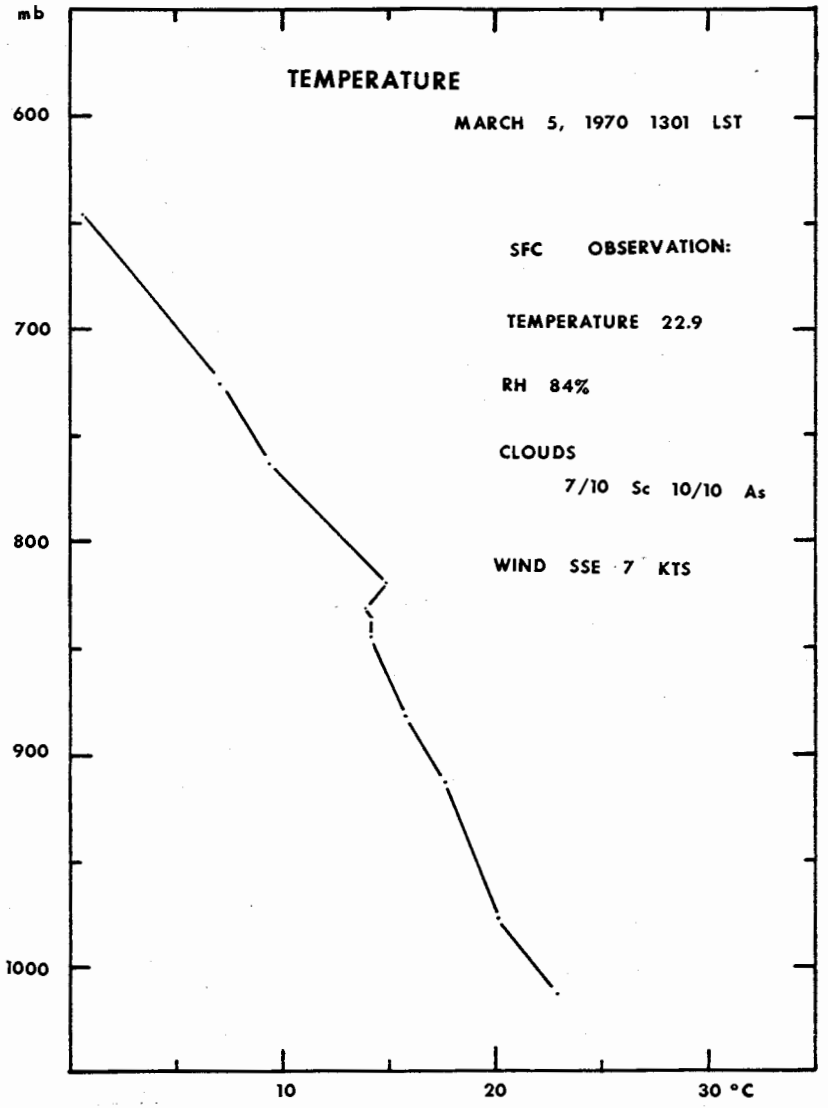

Figure A26. Standard sonde temperature curve.

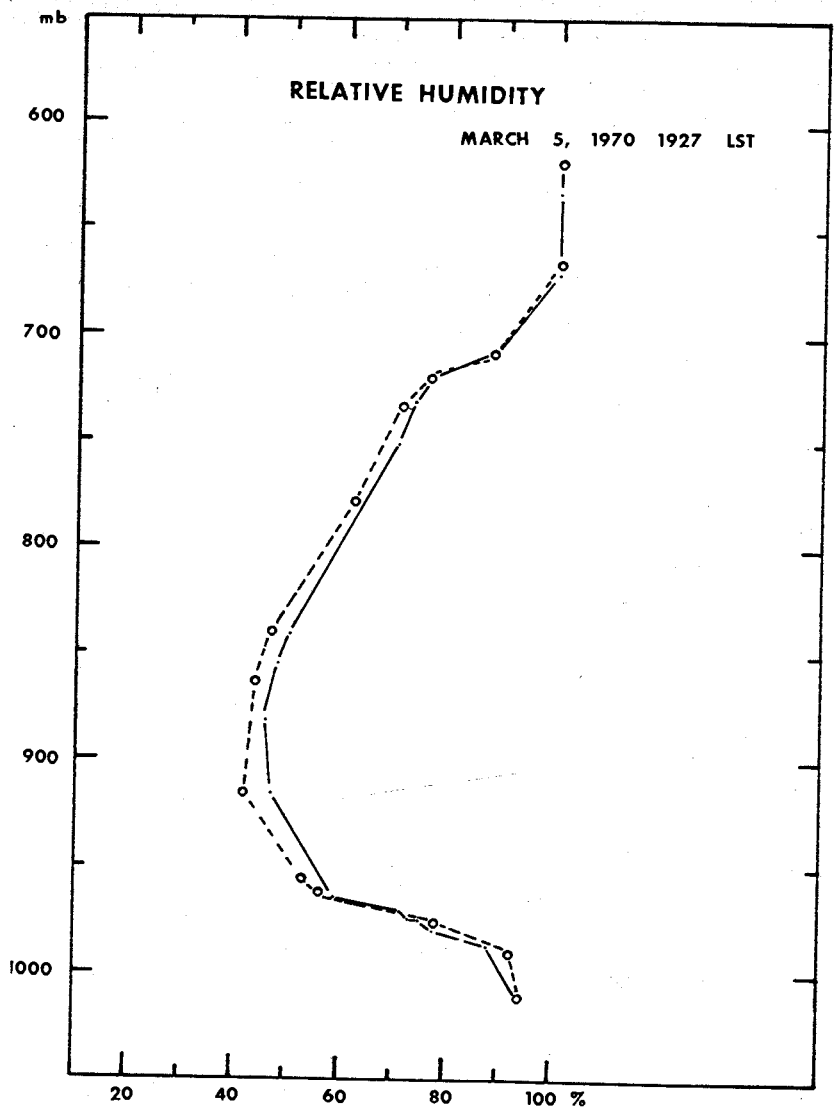

Figure A27. Standard sonde ——— vertical tube -----.

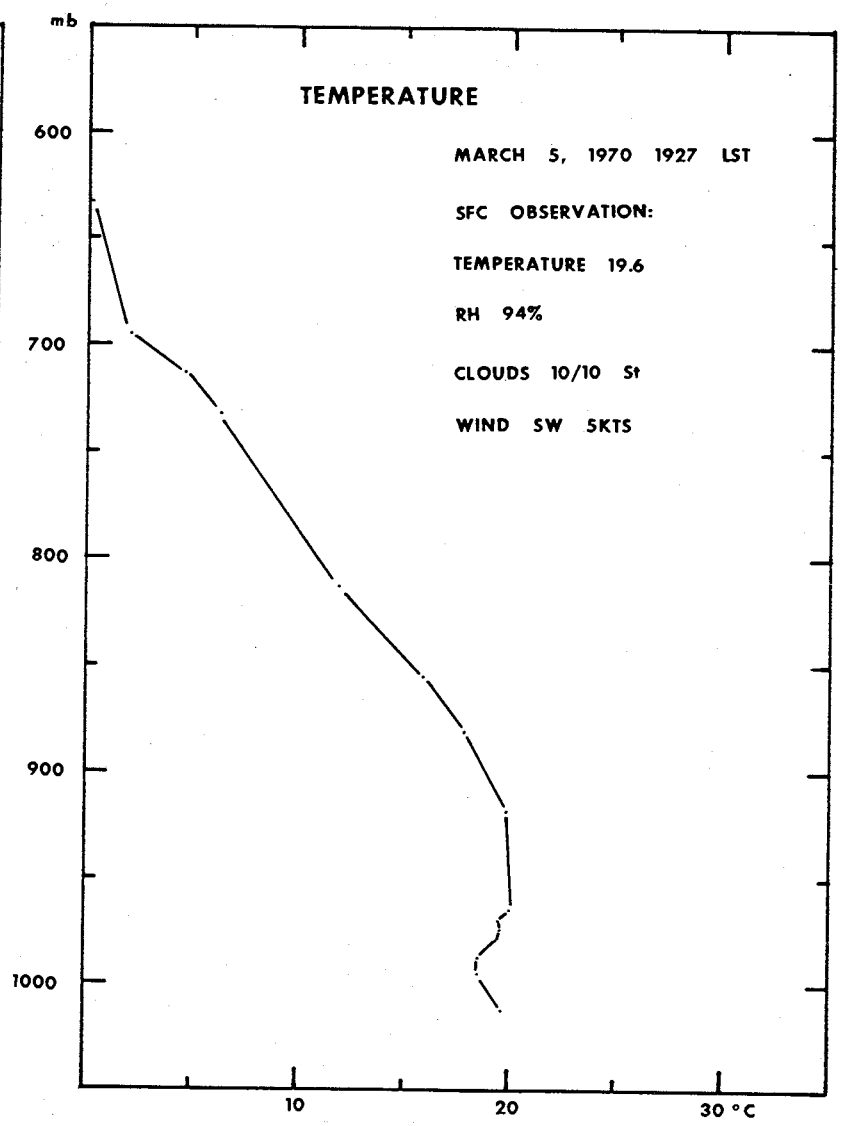

Figure A28. Standard sonde temperature curve.

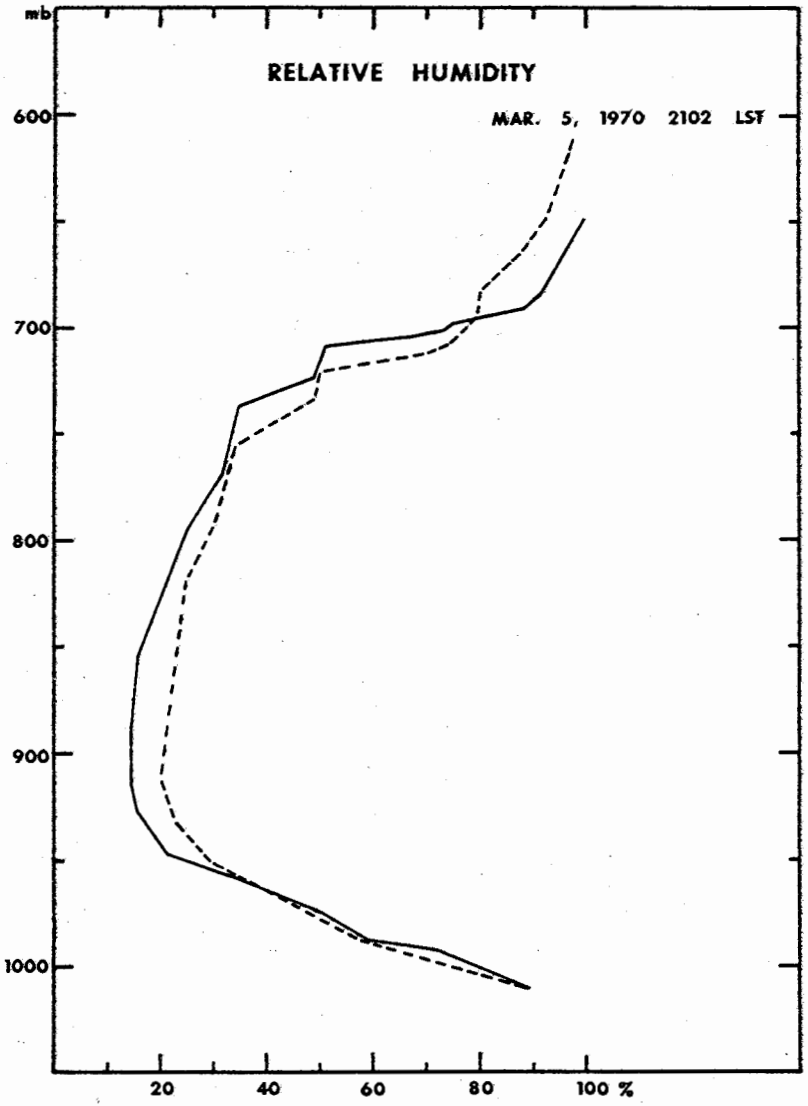

Figure A29. Standard sonde ——— vertical tube -----.

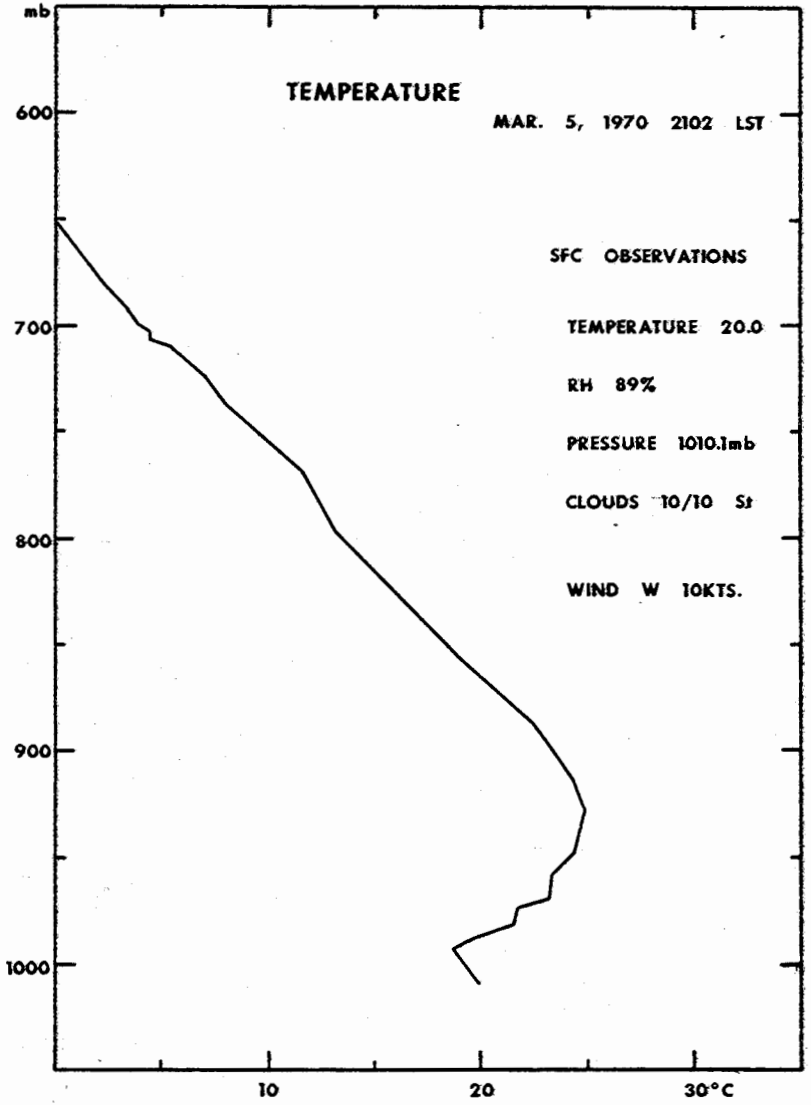

Figure A30. Standard sonde temperature curve.

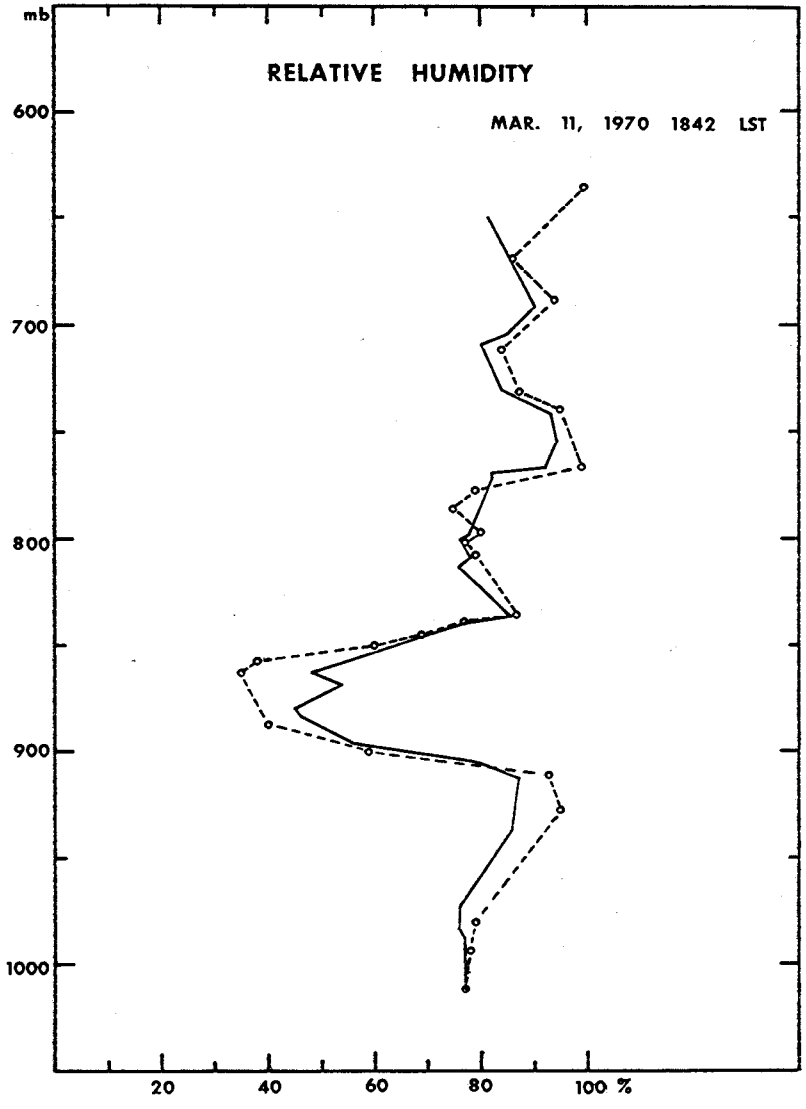

Figure A31. Standard sonde —— vertical tube -----.

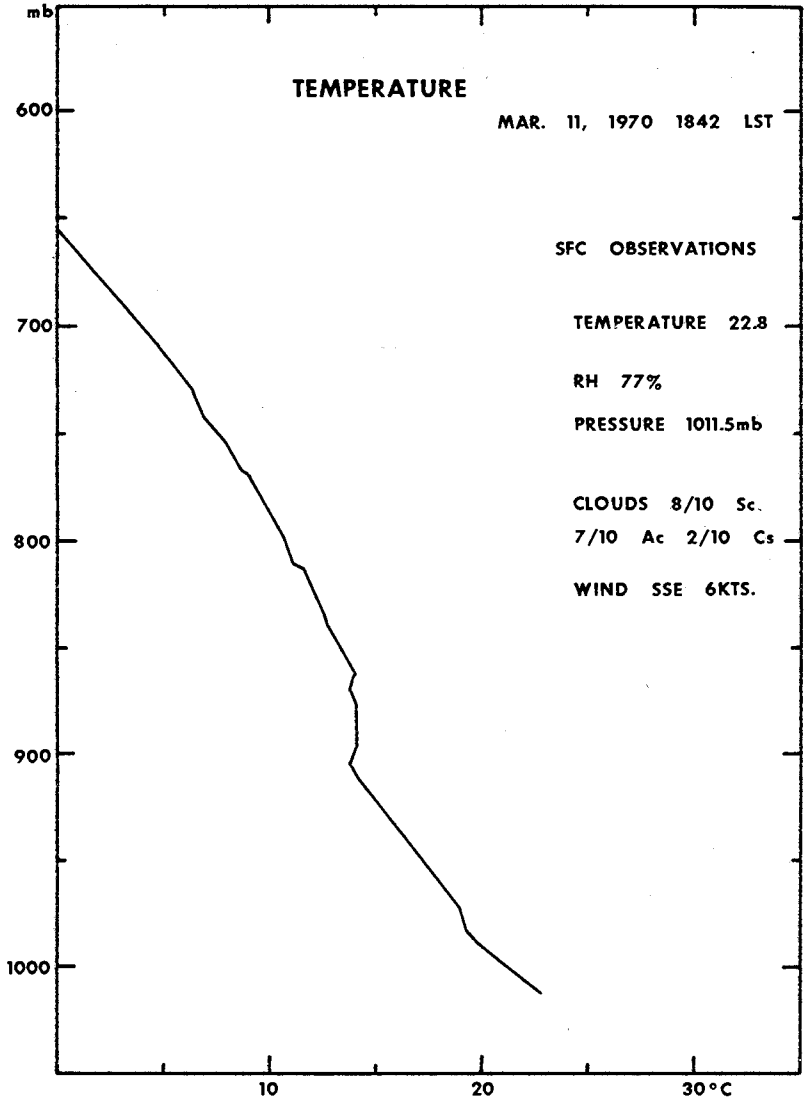

Figure A32. Standard sonde temperature curve.

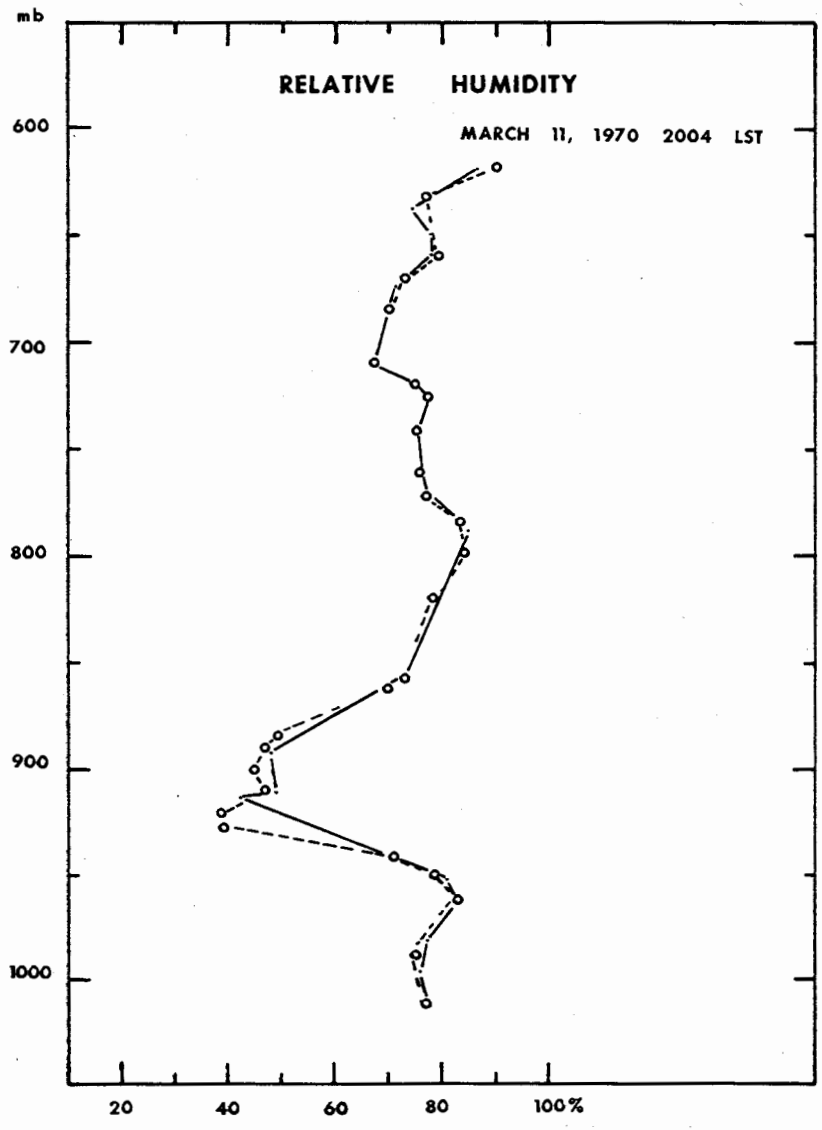

Figure A33. Standard sonde ——— vertical tube -----.

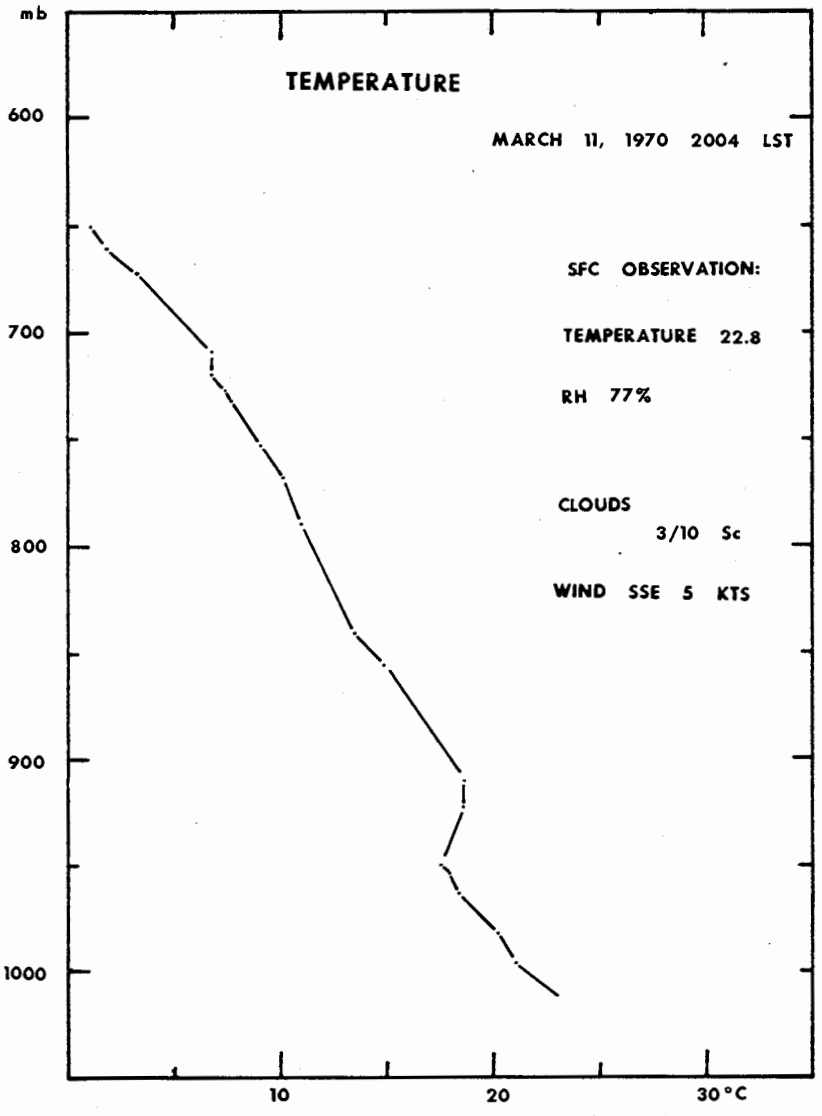

Figure A34. Standard sonde temperature curve.

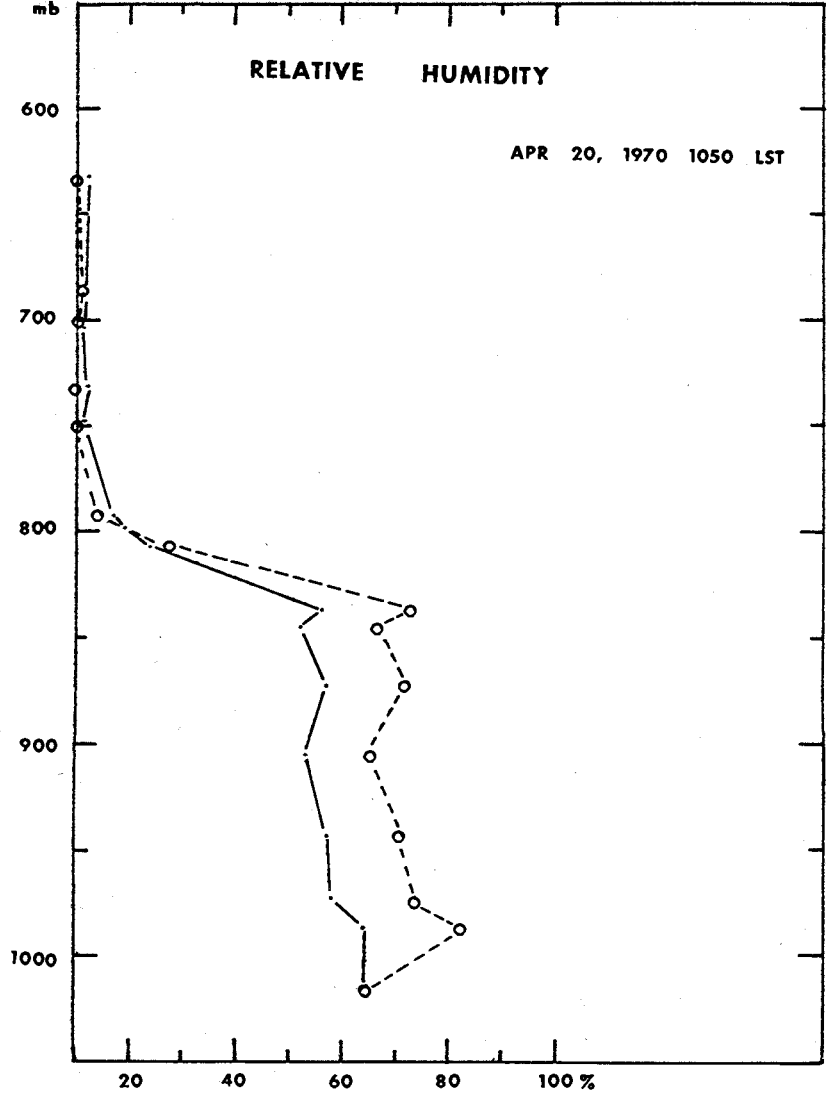

Figure A35. Standard sonde ——— vertical tube and rewired to transmit RH and reference only -----.

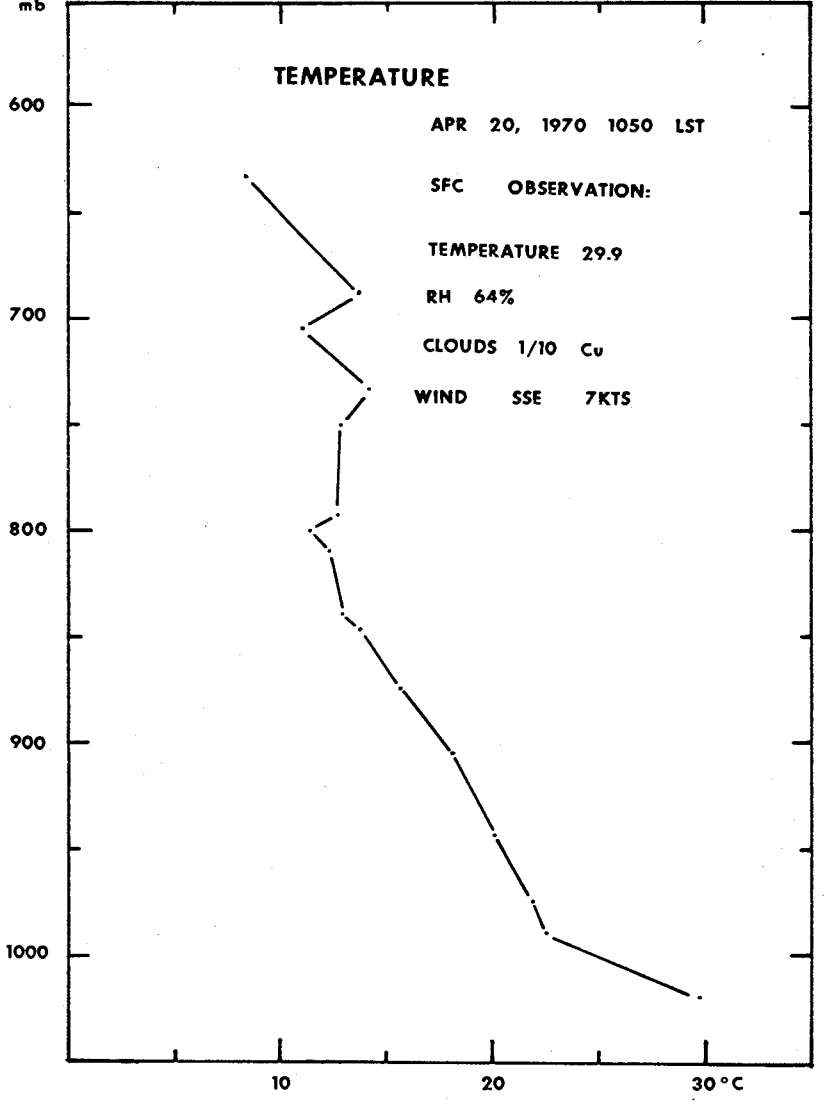

Figure A36. Standard sonde temperature curve.

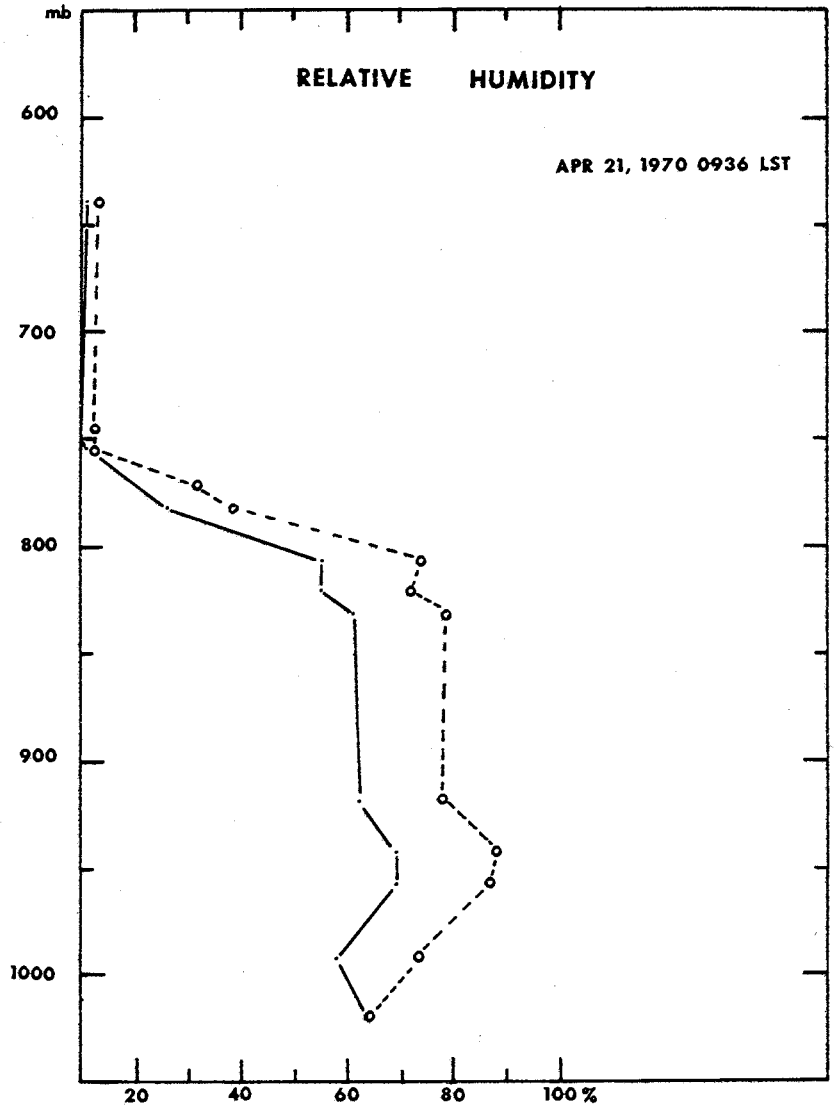

Figure A37. Standard sonde ——— vertical tube and rewired to transmit RH and reference only -----.

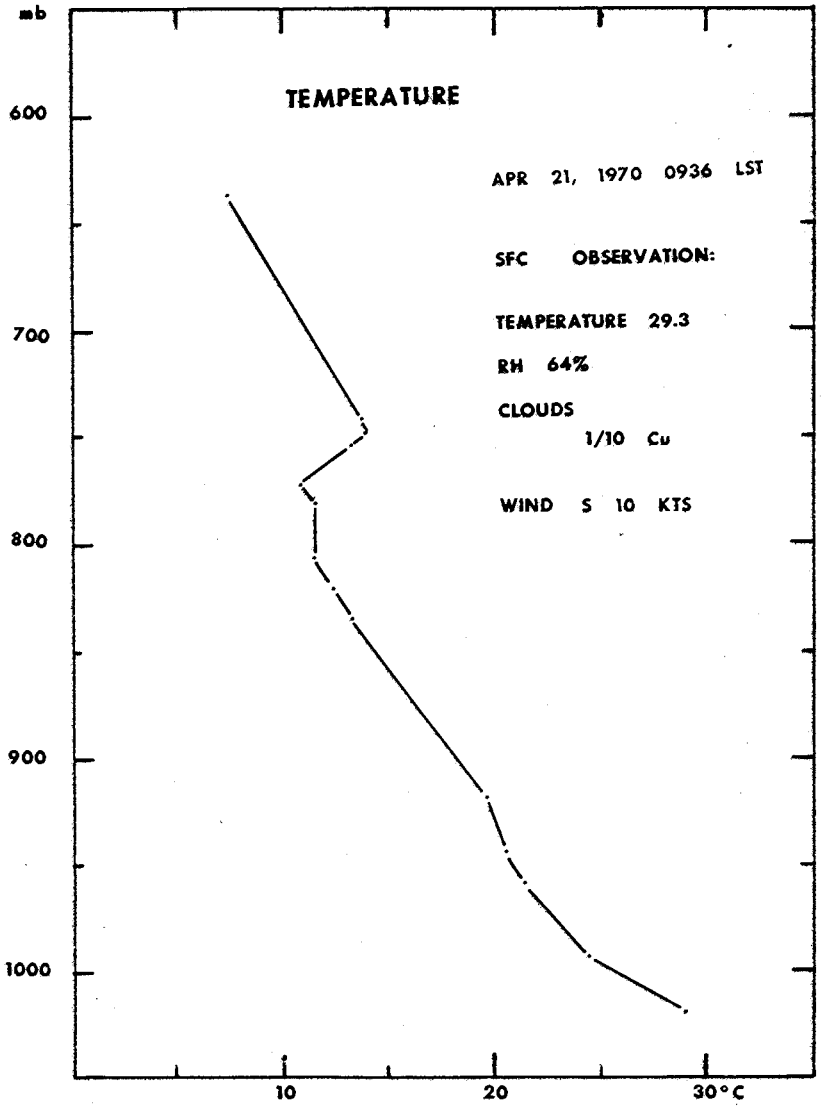

Figure A38. Standard sonde temperature curve.

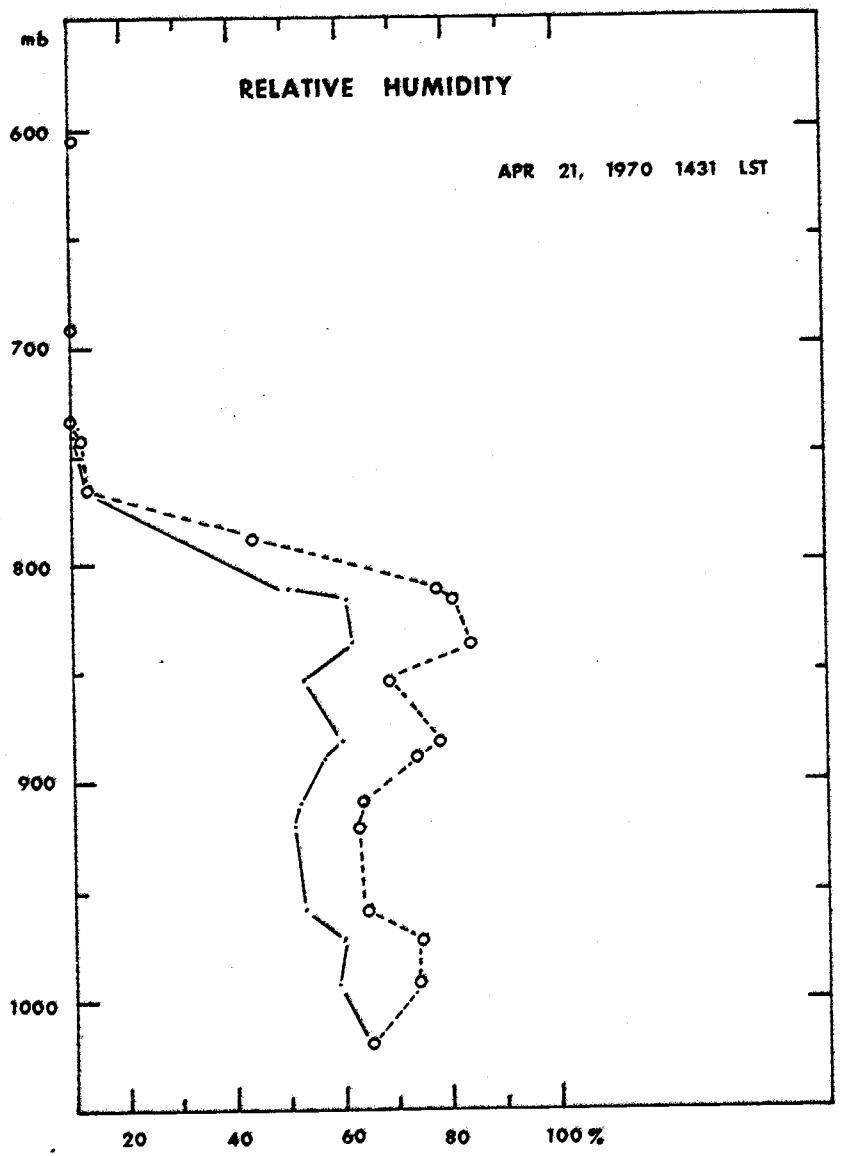

Figure A39. Standard sonde ——— vertical tube and rewired to transmit RH and reference only -----.

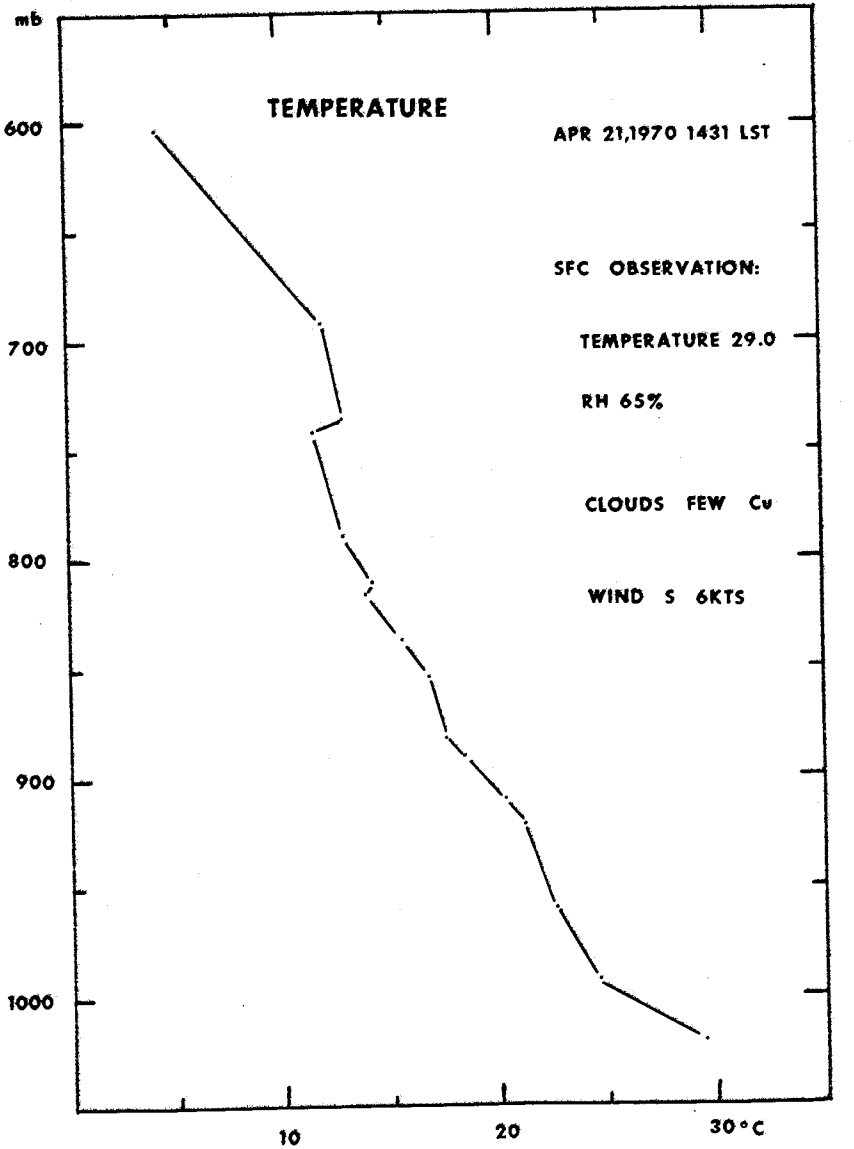

Figure A40. Standard sonde temperature curve.

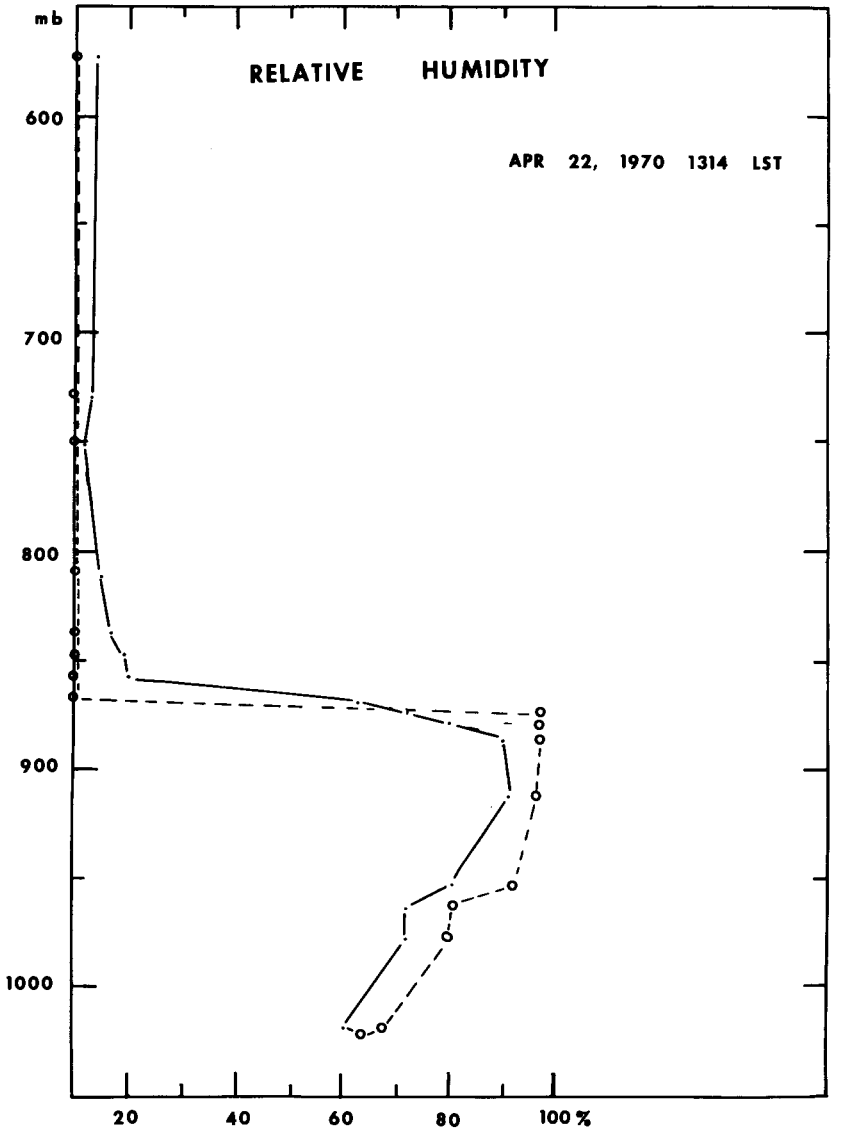

Figure A41. Standard sonde ——— vertical tube and rewired to transmit RH and reference only -----.

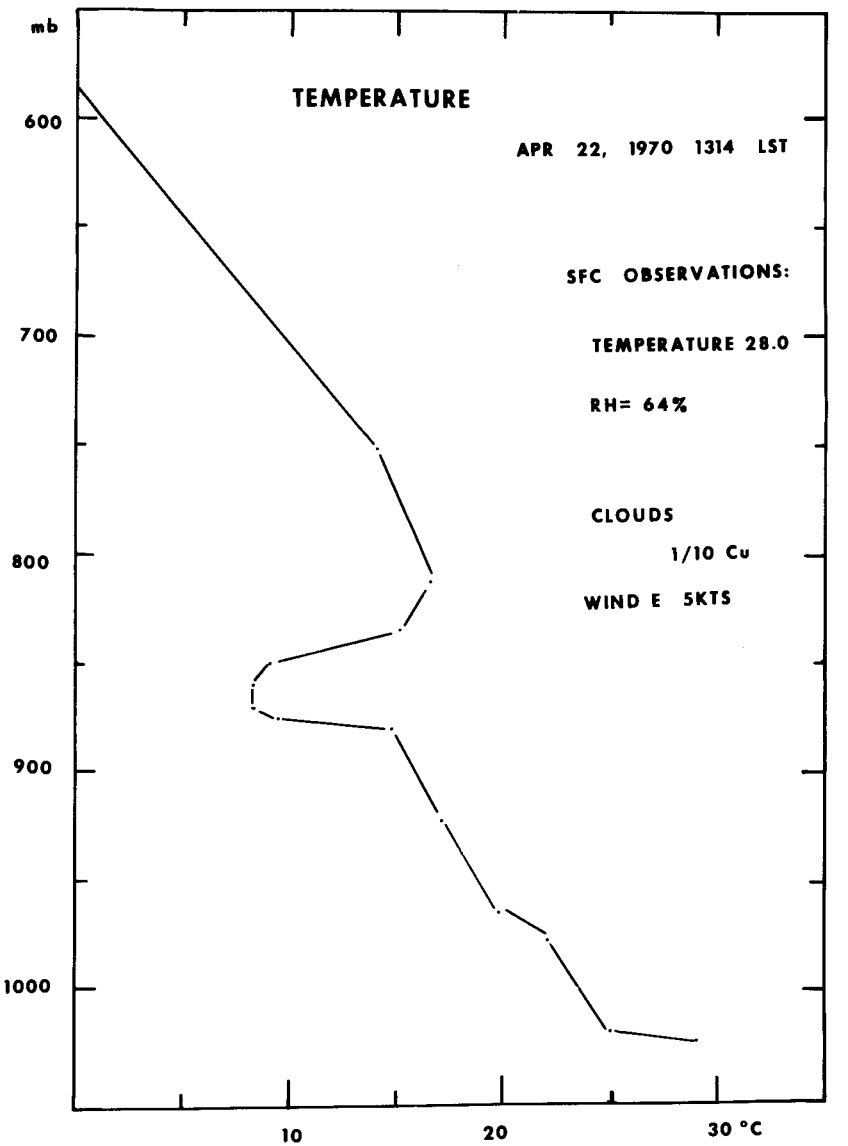

Figure A42. Standard sonde temperature curve.

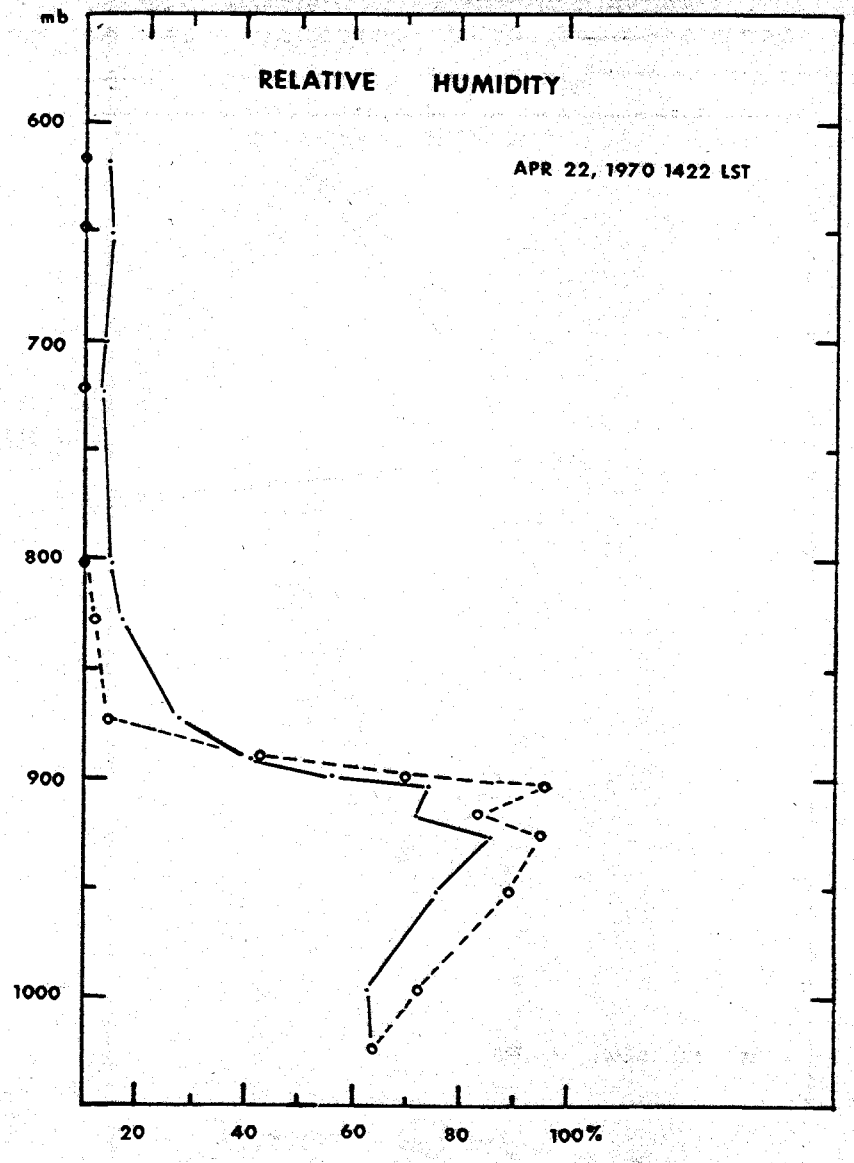

Figure A43. Standard sonde ——— vertical tube and rewired to transmit RH and reference only -----.

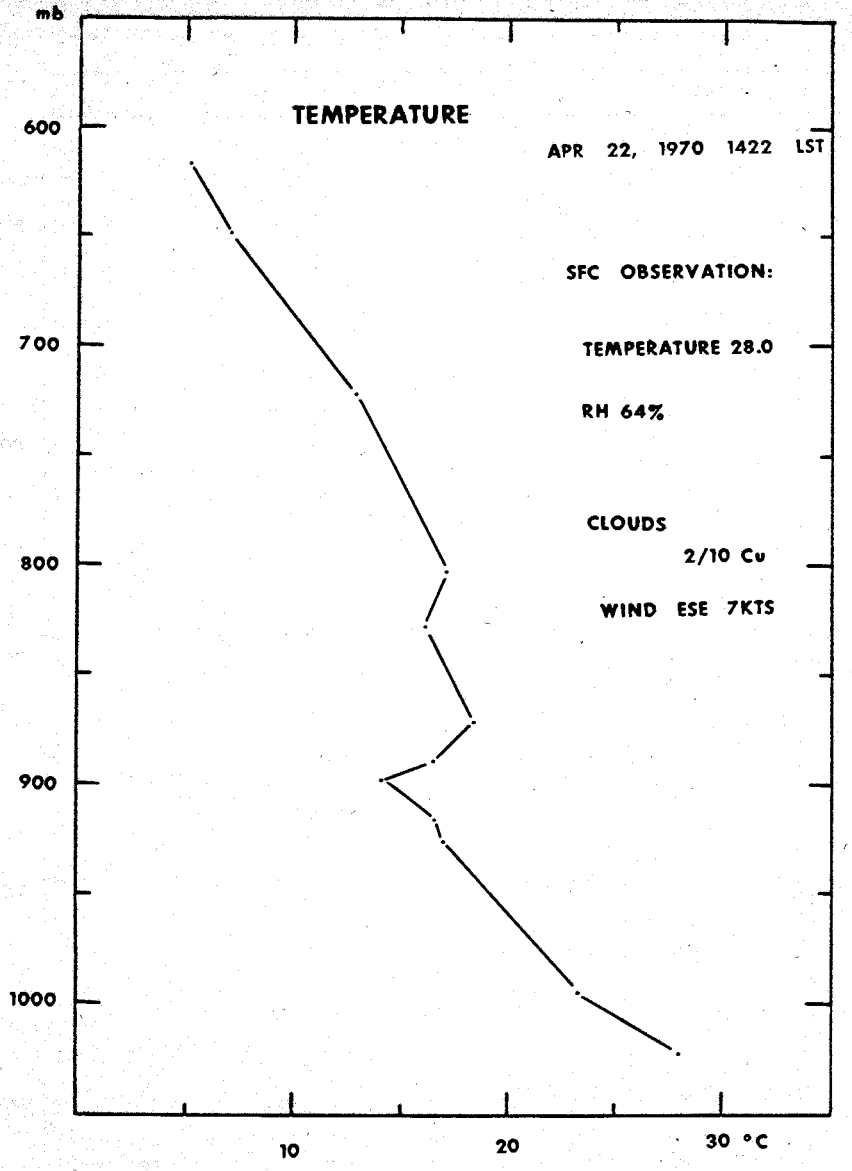

Figure A44. Standard sonde temperature curve.

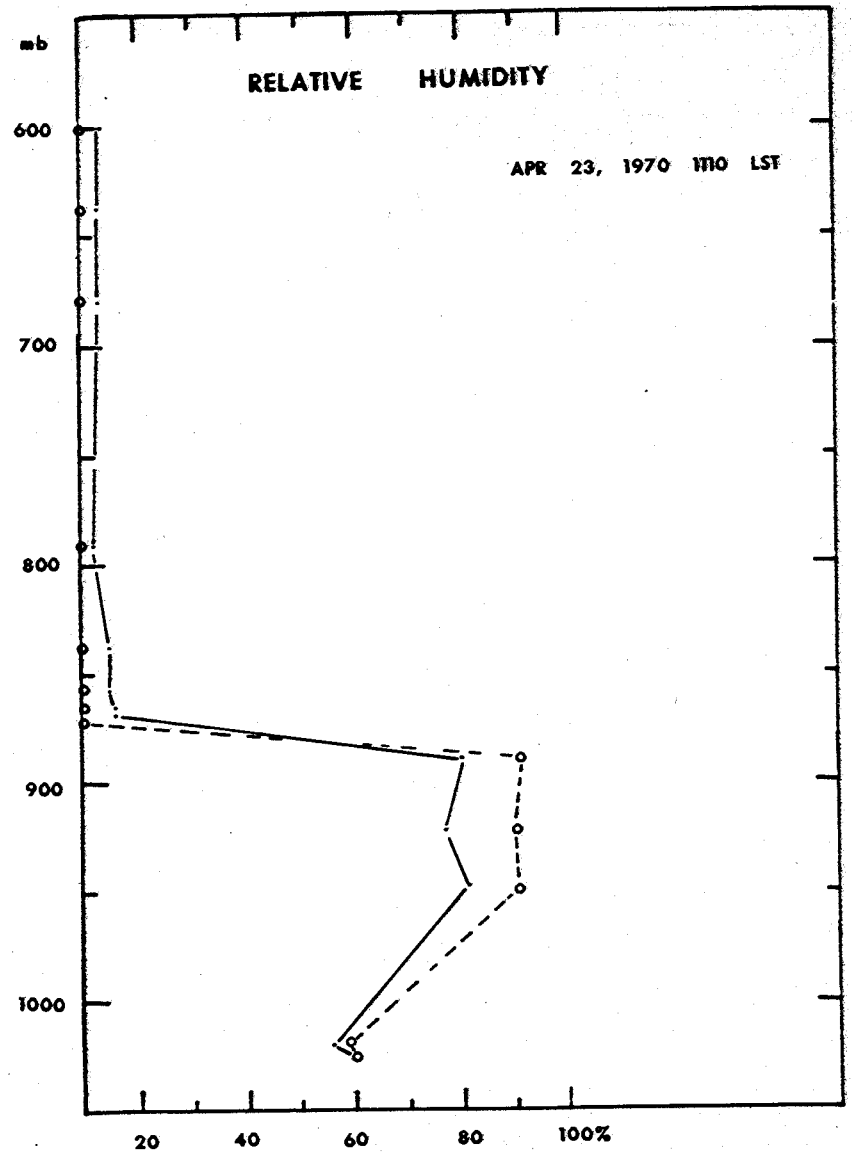

Figure A45. Standard sonde ——— vertical tube and rewired to transmit RH and reference only -----.

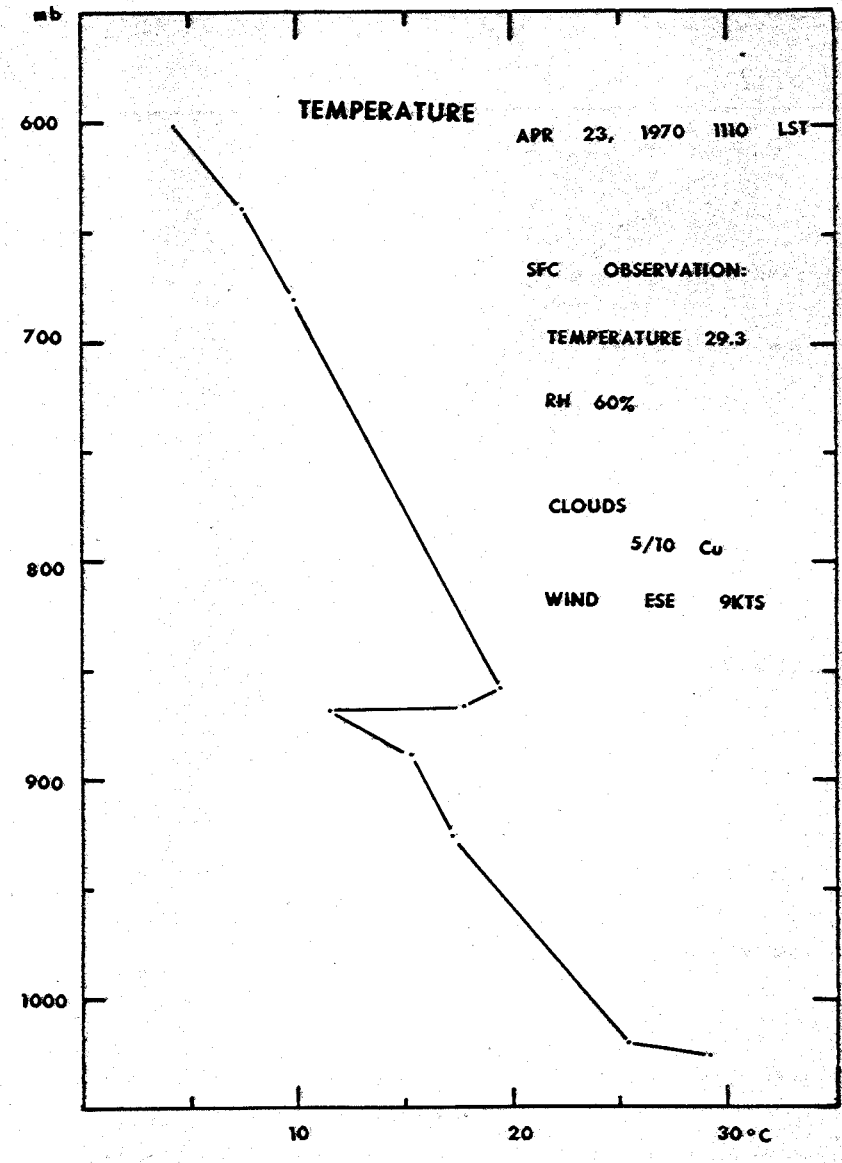

Figure A46. Standard sonde temperature curve.

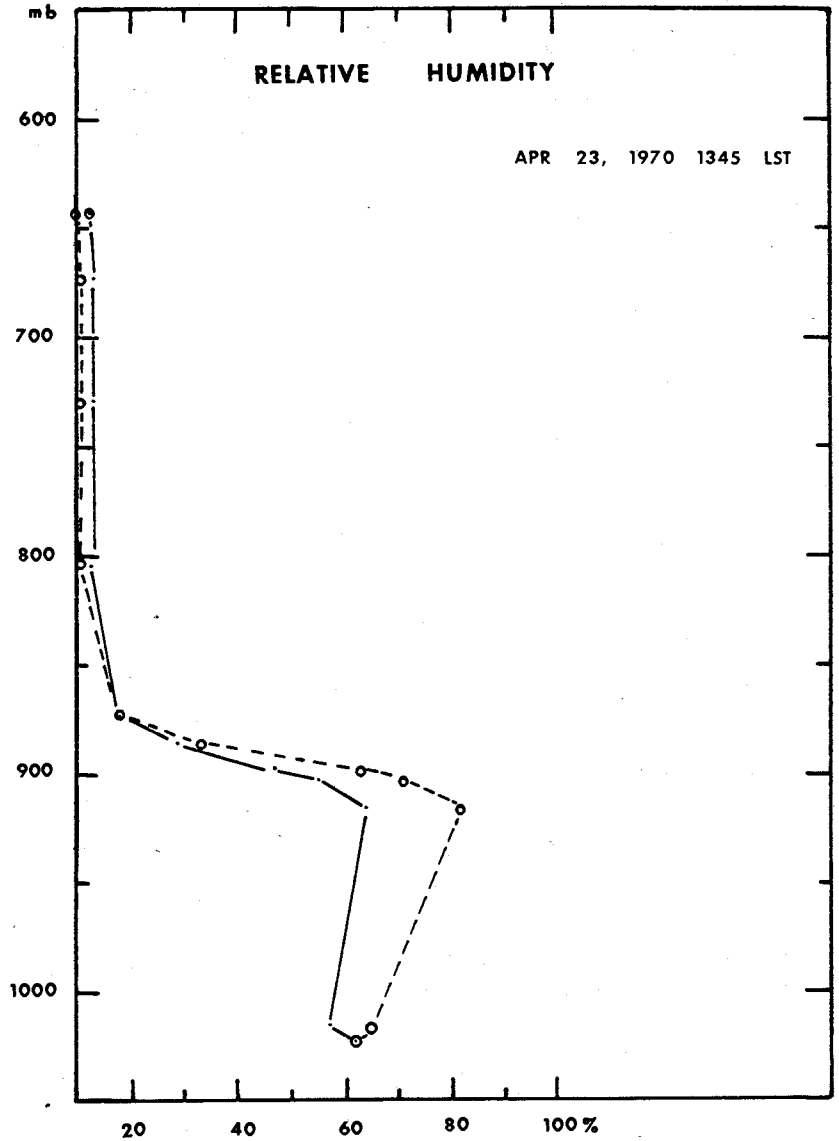

Figure A47. Standard sonde ——— vertical tube and rewired to transmit RH and reference only -----.

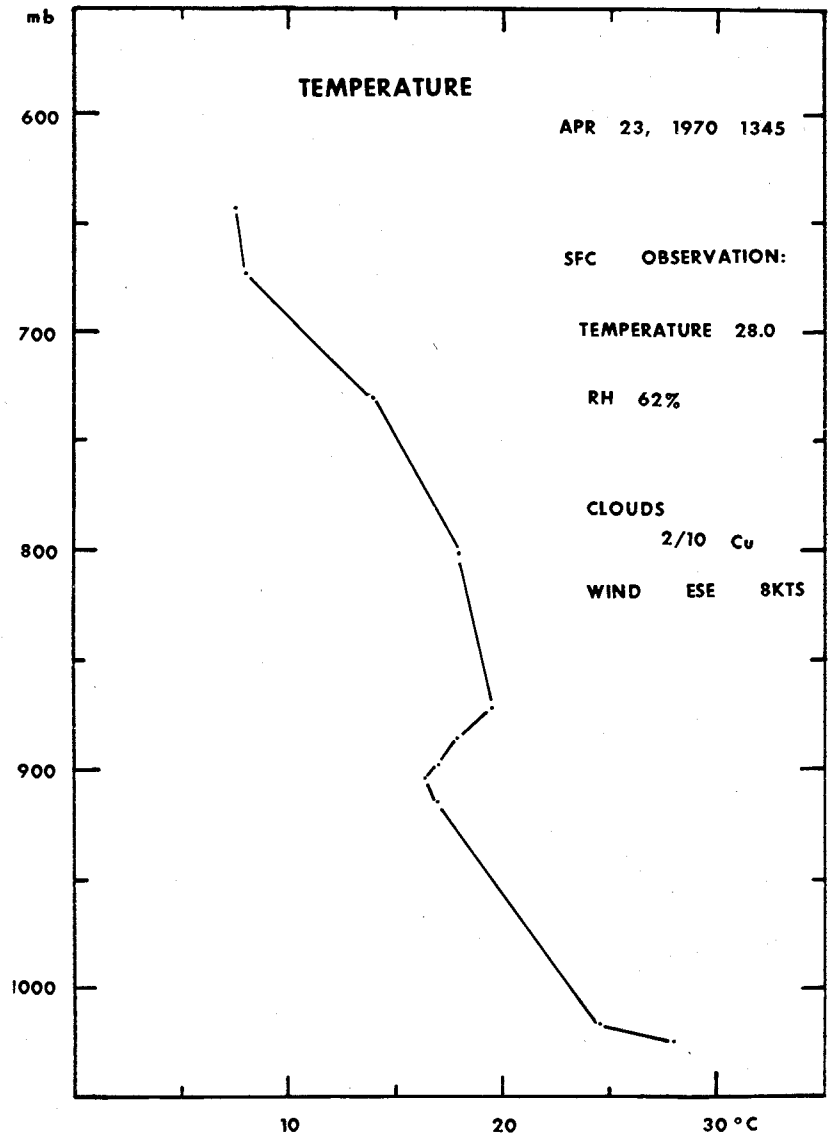

Figure A48. Standard sonde temperature curve.

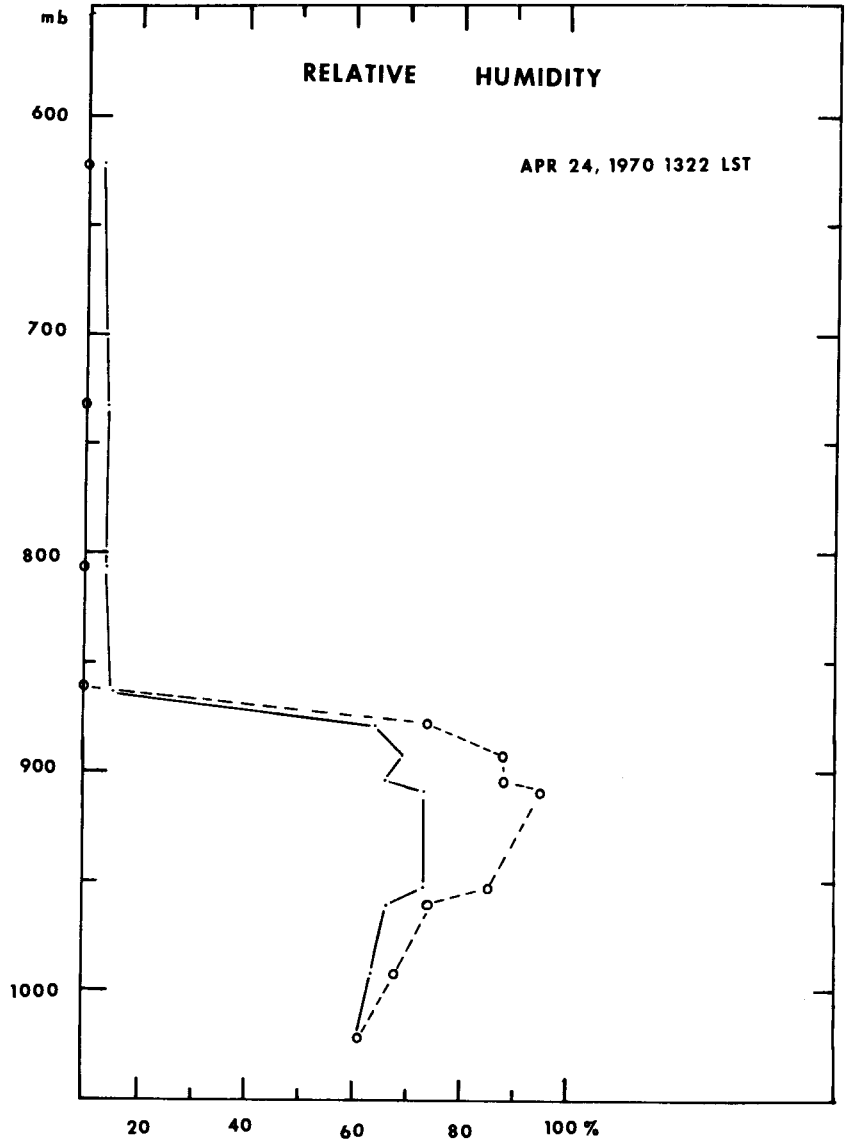

Figure A49. Standard sonde ——— vertical tube and rewired to transmit RH and reference only -----.

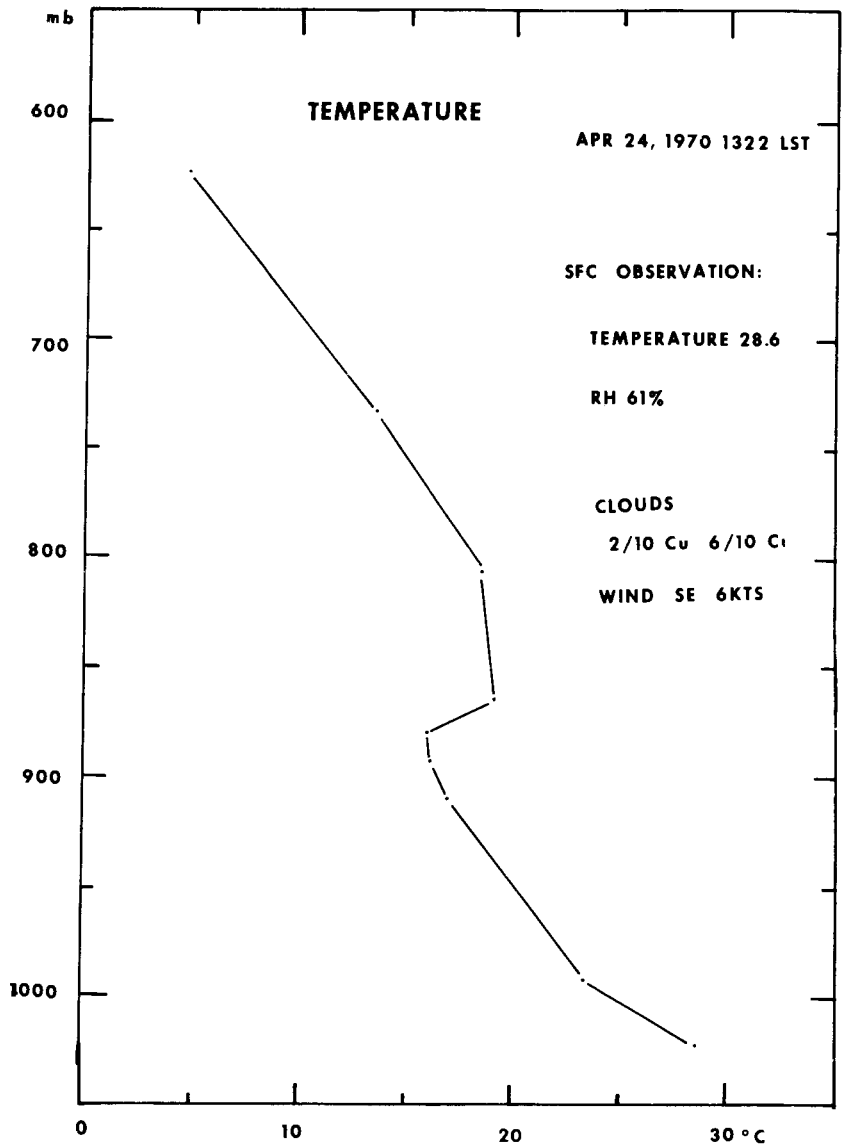

Figure A50. Standard sonde temperature curve.

GPO 833 - 029